Statistical evidence on distinct impacts of short- and long-time fluctuations of Indian Ocean surface wind fields on Indian summer monsoon rainfall during 1991–2014

Yangxing Zheng[1], Mark. A. Bourassa[1, 2], M. M. Ali[1]

[1]*Center for Ocean-Atmospheric Prediction Studies, The Florida State University, Tallahassee, FL, USA*

[2]*Department of Earth, Ocean, Atmospheric Science, The Florida State University, Tallahassee, FL, USA*

Corresponding author address:

Yangxing Zheng

Center for Ocean-Atmospheric Prediction Studies (COAPS), Florida State University, 2000 Levy Avenue, Room 296, Building A, Tallahassee, Florida, 32306

E-mail: yzheng@fsu.edu

Tel: (850) 644-1159

Submitted to *Climate Dynamics*

Submitted in December 2019

Abstract

This observational study mainly examines the impacts of short- and long-time fluctuations of surface wind fields over the Arabian Sea (AS), the Bay of Bengal (BoB), and the southern Indian Ocean (SIO) on Indian Summer Monsoon Rainfall (ISMR), with special reference to strong and weak Indian summer monsoons (ISM). Two datasets over 1991–2014 are used: (1) the daily gridded rainfall produced by India Meteorological Department (IMD), and (2) the Cross-Calibrated Multi-Platform (CCMP) wind product version 2.0 created by Remote Sensing Systems.

Monthly mean surface wind speed, convergence, and curl in the AS, BoB, and SIO are overall not significantly different between strong and weak ISMRs except for wind speed in the AS in September. However, the probability density function (PDF) distribution of daily values over the AS, BoB, and SIO during strong ISMRs is different from during weak ISMs, suggesting that sub-monthly surface wind characteristics could be useful in diagnosing rainfall characteristics. Except for rainfall in the northeast part of India, Indian regional rainfalls are closely linked with surface wind speeds over the AS, and wind convergence and curl over the BoB on short timescales of up to one week. The daily area-averaged wind convergence over the BoB is better correlated with regional rainfall during strong ISMs than during weak ISMRs. Multiple linear regression analysis shows that the fluctuations of monthly wind fields in the AS and BoB can affect monthly rainfall in some regions but are not related to a significant change in rainfall over the whole India. It is the short-time fluctuations of wind speed over the AS as well as wind convergence and curl over the BoB rather than their long (monthly) timescale fluctuations that are related to the strength of ISMR. Surface winds over the SIO on weather timescales have little influence on ISMR.

Keywords: Indian summer monsoon rainfall, CCMP surface winds, Indian regional rainfall

1 Introduction

Indian summer monsoons (ISMs) have a tremendous effect on the well-being of residents in India and neighboring countries. The strength of ISMs is often measured by the All-India summer rainfall index (AIRI) represented by the amount of Indian summer monsoon rainfall (ISMR) seasonally (June–September, or JJAS) averaged across all of India (Parthasarathy et al. 1992). ISMR has two erratic natures: 1) the "bursting" of a monsoon characterized by an abrupt change in the mean daily rainfall (Allaby 2002) and 2) the "vagaries" of rainfall variability in time and space in India (Parthasarathy et al. 1990; Kulkarni et al. 2006). As the mechanisms behind these two features are not yet completely understood, ISMR is notoriously difficult to predict. This study is an effort to understand the mechanisms controlling the strength of ISMR by focusing on the investigation of how Indian Ocean surface winds on short and long timescales affect the strength of ISMR. Several early studies (Verma and Kamte 1980; Joesph et al. 1981; Parthasarathy et al. 1991) indicated a good relationship between 200-hPa meridional winds in May and Indian monsoon rainfall and further discussed its potential for predicting the Indian seasonal rainfall. The interannual variations of ISMs have also been described in terms of several circulation indices in terms of wind fields, including Webster and Yang monsoon Index (WYI; Webster and Yang 1992), Monsoon Hadley Circulation Index (MHI; Goswami et al. 1999), convection index (CI; Wang and Fan 1999), and a unified monsoon index defined by dynamical normalized seasonality (DNS; Li and Zeng 2002). Thus, ISMR variations are associated with variations of high level (e.g., 200 hPa) and low level (e.g., 850 hPa) wind fields. For example, Govardhan et al. (2017) suggested that the meridional shear of 200-hPa winds between the subtropical westerly jet stream and tropical easterly jet can cause a barotropic instability in a monsoon basic flow (to form synoptic disturbance) that controls the revival of the summer monsoon subsequent to the break events. During the boreal summer, ISM surface circulation is predominantly controlled by southwest winds in the northern Indian Ocean. These winds, known as an atmospheric western boundary current, are strengthened by the high terrain over eastern Africa. Therefore, it is believed that the "vagaries" of ISMR are closely linked with the temporal and spatial variability of surface winds over the Indian Ocean. This study focuses on the impacts of surface winds in the Indian Ocean on ISMR on short (sub-monthly) and long (monthly) timescales. We will show that long timescale mean winds are a poor diagnostic for rainfall characteristics, and that the distribution of winds based on shorter (daily) timescales is a much better diagnostic.

Many basin-scale factors such as Indian Ocean dipole (IOD) and several global phenomena including tropical intraseasonal oscillation (ISO), the El Niño Southern Oscillation (ENSO), the Atlantic Multi-decadal Oscillation (AMO), the Pacific Decadal Oscillation (PDO), large-scale land-surface processes (e.g., Eurasian snow cover), and the total solar irradiance (TSI) also influence ISMR through modulating surface winds and the associated moisture on a wide range of timescales. For example, many studies have suggested that the "bursting" and "vagaries" of ISMR are connected with the "active (wet spells)" and "break (dry spells)" phases of an ISM and the associated wind patterns can be greatly influenced by the tropical ISO (Yasunari 1979; Sikka and Gadgil 1980; Lau and Chan 1986; Krishnamurthy and Shukla 2000). The impacts on ISMR from these global phenomena are usually interwoven and complex. For example, the variability of ISMR can be greatly influenced by ENSO on interannual timescales (Shukla 1987), although ENSO's impacts can be concealed or masked by other important factors such as IOD, ISO, PDO, and Eurasian snow cover, leading to an unclear link between ENSO and ISMR. Eurasian snow cover has been confirmed to play a critical role in subsequent ISMR (Blanford 1884; Dey and Bhanu Kumar 1982, 1983; Dickson 1984; Vernekar et al. 1995). PDO usually affects ISMR on decadal to interdecadal timescales (Malik et al. 2017, 2018) and the deficit (excess) rainfall in India is tied to the warm (cold) phase of the PDO by changing Hadley circulation in the monsoon region (Krishnamurthy and Krishnamurthy 2014). Venugopal et al. (2018) concluded that the ocean mean temperature, representing the thermal energy available in the ocean, of the southwestern Indian Ocean spanning from 10°S to 0° and 50°E to 70°E has a success rate of 80% in predicting stronger or weaker than average ISMR compared to the existing atmospheric and oceanic indices.

As a low branch of monsoonal circulation, the temporal and spatial changes of the prevailing southwest winds in the Indian Ocean have an essential impact on the strength of an ISMR in several ways. First, these winds are the major force driving the underlying ocean circulation dynamically and thermodynamically. For example, southwest winds produce eastward surface currents owing to the Coriolis effect driving the upper ocean circulation and exchanging the upper water of different temperatures between the western and eastern parts of the Indian Ocean. This significantly changes the spatial distribution of the upper ocean temperature and sea surface temperature patterns via oceanic dynamics and surface heat flux, causing a shift in the IOD and ocean water evaporation (i.e., moisture in the air). The IOD, an irregular fluctuation in sea surface temperature between western and eastern Indian Ocean, is closely linked with ISMR: positive (negative) IOD is generally conducive to the strong (weak) ISMR (e.g., Ashok et al. 2001; Sreejith et al. 2015). Additionally, the temporal and spatial variations of surface wind speed, convergence, and curl in the Indian Ocean, particularly in the Arabian Sea (AS) and the Bay of Bengal (BoB) are believed to be critically important to the transport of moisture (i.e., moisture-laden winds) to the Indian subcontinent (Sadhuram and Ramesh Kumar 1988; Levine and Turner 2012). It is this transport of moisture that fuels convection and storm cloud development over land, a precursor to the formation of precipitation in India. Konwar et al. (2012) revealed that an increasing trend of low-level wind speed and moisture content over the AS contributes to an increasing trend of vertically integrated moisture transport over the AS, while a decreasing trend of low-level wind speed and moisture content over the BoB contributes to a decreasing trend of vertically integrated moisture transport over the BoB, leading to an east-west asymmetry of ISMR trend in the past three decades. The water vapor flux over the southern Indian Ocean (SIO) crossing the equator is also believed to be one of the main moisture sources for ISMR (Cadet and Greco 1987a, b), and therefore the variations of winds over the SIO are also presumed to affect the strength of ISMR. Since surface wind speeds along the Somali coast (SC), as part of the Somali Jet, are high and have high variability (Findlater 1969), they can affect the SST distribution and drive winds over the AS towards India at a greater pace and intensity. In addition, winds over the eastern Indian Ocean (EIO) may be more important for IOD formation and consequently influence the ISM (Krishnan and Swapna 2009). Here, wind features over the SC and EIO will also be analyzed and their association with Indian rainfall will be compared to that over the AS and SIO, respectively. Furthermore, land-sea breeze is an important process for precipitation in coastal regions. Thus, the features of surface winds in time and space over the Indian Ocean are believed to substantially affect the strength of ISMR.

That said, several basic but important issues regarding the links between ocean surface winds and India's rainfall variability remain unresolved. These questions include, but are not limited to: (a) Is the strength of ISMR determined by the strength of surface winds? If so, on what temporal scales (e.g., daily, weekly, or monthly), at what locations and with what wind characteristics (wind speed, convergence, and curl), can surface winds evidently influence and/or be strongly related to the rainfall over entire India and/or regional rainfall? (b) Do these impacts differ during strong and weak ISMRs? Answering these questions would greatly advance our understanding of ISMR. This study is an attempt to answer these questions based on high-quality observations. To study the links of the regional rainfall with winds, we choose the rainfall over the homogeneous rainfall zones of India as regional rainfall. The India Meteorological Department (IMD) defines four homogeneous rainfall zones to represent geographical distribution of regional Indian rainfall. These four homogeneous rainfall zones are northwest India (NWI), northeast India (NEI), central India (CI), and south peninsula (SPIN), shown in Fig. 2 of Zheng et al. (2016b)). In this study, we simply call these four regions as the IMD regions. The IMD regions have been selected for analysis in several studies (e.g., Pattanaik 2007a, b; Zheng et al. 2016a, b).

Zheng et al. (2016a) studied the monthly and regional rainfall contribution to the overall ISMR and Zheng et al. (2016b) studied how the rainfall in different regions varies during strong and weak ISMs. Saha et al. (2019) suggested that the internal variability of ISM caused by subseasonal (synoptic and intraseasonal) fluctuations is partly predictable owing to its association with slowly varying forcing such as ENSO, intimating the significance of short timescale fluctuations in the strength of ISMR. In this study, we go further to study the impacts of short- and long-time fluctuations of Indian Ocean surface winds on ISMR. We focus on investigating the characteristics of the observed daily surface winds in each month of summer monsoon seasons (i.e., June through September, JJAS) between strong and weak ISM years. Four surface wind fields—surface wind vector, wind speed, wind convergence, and curl—over the Indian Ocean are examined. These four wind fields are assumed to be relevant to rainfall variability over the Indian subcontinent. Distinctive monthly wind features between strong and weak ISM years will be first identified, whenever and wherever they exist. Implications of these distinctive surface winds with regard to the rainfall variability in the IMD regions will also be discussed. It should be pointed out that whether these distinctive surface wind features are related to basin-scale phenomena (such as IOD) and global phenomena (such as ENSO, PDO, Eurasian snow cover, TSI) is generally focused on interannual to interdecadal timescales, and these are beyond the scope of the present study, partially owing to the short record of data used in this study as described in the methodology section. A separate study should be conducted to address these issues.

The rest of this work is organized as follows. Section 2 briefly describes the methods and datasets. The detailed results are presented in section 3. Discussion regarding the roles of monthly mean surface wind fields over the AS, BoB, and SIO in the strength of ISMR is presented in section 4. Section 5 concludes the paper and includes some caveats and perspectives for future study.

2 Methods and data

2.1 Methodology

In this study, the daily all-India rainfall (AIR) was obtained by area-averaging the IMD's daily gridded (1° × 1°) rainfall, and the ISMR for each year was then computed as the sum of daily AIR from June 1 to September 30 (referred to as JJAS rainfall hereafter). The strength of an ISM, represented by the magnitude of ISMR, is defined in the same way as in our previous study (Zheng et al. 2016b): a strong (weak) ISM is when the ISMR is greater (smaller) than 110% (90%) of the JJAS rainfall climatology computed over the period 1951–2014. This definition of a strong (weak) ISM year is consistent with the definition of IMD "excess" ("deficient") rainfall year when the rainfall of the particular year is greater (smaller) than 10% of the long-term mean. Fig. 1 shows the JJAS rainfall area averaged over all India and the four IMD regions during 1991–2014. There are three strong ISM years (2005, 2007, and 2008), three weak (2000, 2002, and 2009) and 18 normal ISM years. It should be noted that weak ISMs in 2002 and 2009 are associated with El Niño, ISMs in 2000 and 2007 are influenced by La Niña events and strong ISMs in 2005 and 2008 are not associated with any ENSO phenomena. Comparisons of all-India JJAS rainfall (Fig. 1a) distribution with the distributions of regional rainfall in the four IMD regions (Fig. 1b–1e) suggest that the total India JJAS rainfall is more associated with the rainfall in NWI and CI, consistent with the results of our previous studies with a long record of rainfall data (Zheng et al. 2016a, b).

Observational features of monthly and seasonally mean rainfall spatial distribution in India during strong and weak ISM years defined in the previous paragraph are first examined based on a composite analysis. Whether monthly and seasonally mean surface wind fields over the Indian Ocean are distinct between strong and weak ISMs is then investigated using a composite method. A composite approach is used with the underlying assumption that the dominant features of the samples behave in a similar manner and are governed by the same mechanisms. Of course, it is very unlikely that all samples/events behave in the same or similar way and that they occur because of the same mechanisms; however, the composite approach is adopted as a first means of identifying the dominant features that potentially behave in a similar manner and are governed by the same mechanisms. In fact, a composite approach is often used to seek common features of some fields (e.g., rainfall, winds) regarding strong and weak ISM periods (Zheng et al. 2016a, 2016b).

To highlight the salient features of daily surface wind fields (wind speed, convergence, and curl) between strong and weak ISMRs, we have applied a probability density function (PDF) approach to the daily surface wind fields. The PDF is used to specify the probability of the variables (e.g., surface wind speed, convergence, and curl) falling within a particular range of values. Through the PDF analysis, it is easy to identify if any dominant modes of daily surface wind fields exist in a particular region during strong ISM years and convey if they are distinguished from those during weak ISM years as well as during normal ISM years.

To examine the relationship between daily fluctuation of ocean surface winds in the AS, BoB, and SIO as well as rainfall variations in the four IMD regions, we perform a simple linear lag correlation analysis to describe the potential links between daily surface wind fields and daily rainfall in the IMD regions.

2.2 Multiple linear regression

To examine the relative roles of monthly wind fields in the AS, BoB, and SIO during the Indian summer monsoon periods, we use a multiple linear regression (MLR) approach to estimate the anomalous monthly rainfall in the entire India and the four IMD regions from anomalous monthly wind fields (wind speed, convergence, and curl) with the following MLR model:

$$Y = a_0 + \sum_{i=1}^{9} a_i X_i + \varepsilon \qquad (1),$$

where Y is the anomalous monthly rainfall in all-India and the four IMD regions, X_i is the ith component (i.e., wind speed, wind convergence, curl in the AS, BoB, and SIO), a_i is the regression coefficient for the ith component, a_0 is intercept, and ε is the estimated error due to linear regression.

2.3 Data

Two major datasets are used in this study: (1) the IMD daily gridded (1°×1°) rainfall product for the Indian subcontinent over 1951–2014 (Pai et al. 2016), and (2) Cross-Calibrated Multi-Platform (CCMP) ocean surface wind velocity products version 2.0 over 1991–2014 (Atlas et al. 2011).

The IMD daily gridded rainfall is well-suited to this study because the daily mean rainfall is able to quantify the rainfall variability on short timescales (e.g., up to one week) as compared to monthly rainfall products, which are not as appropriate. In addition, this rainfall product can be used to produce rainfall in separate homogeneous rainfall zones of India as regional rainfall, and thus allows us to examine the links of regional rainfall with surface winds in the Indian Ocean on short timescales (i.e., up to one week).

CCMP V2.0 wind product contains four maps (at 00, 06, 12, 18Z) on a $0.25^{o} \times 0.25^{o}$ grid from July 1987 through May 2016. Since data before 1991 is insufficient, data over the period 1991–2014 are used in this study. Using a variational analysis method, the CCMP wind product was derived from several sources of wind observations such as moored buoy wind data, Version-7 Remote Sensing Systems radiometer wind speeds, ASCAT and QuikSCAT scatterometer wind vectors, and the European Center for Medium-Range Weather Forecast (ECMRWF) ERA-Interim model wind fields (Atlas et al. 1996, 2011; Hoffman et al. 2003). CCMP winds are referenced to 10 m above surface. This wind product is selected because the wind data are of the high quality with high temporal and spatial resolutions, which are well suited to studying the wind characteristics at fine scales in both space and time. For this study, we choose the period 1991–2014 for analysis of winds and rainfall. A detailed description of the CCMP product can be found at http://www.remss.com/measurements/ccmp. It should be noted that although this version of the CCMP wind product has several advantages, it also has some known issues. For example, this wind product may be suitable for studying region trends and patterns, but it is not well-suited for studying global trends because bogus trends in the background wind field can be created from assimilation processes. In addition, high wind speeds (> 25 m s^{-1}) should be used cautiously because high wind events are known to be underestimated by the background model.

3 Results

The geographic distributions of monthly and seasonal mean rainfall between strong and weak ISMs are first described in section 3.1. If monthly and seasonally mean surface wind fields in the Indian Ocean are significantly distinct between strong and weak ISMs, then the monthly variations (i.e., long-time fluctuations) of surface wind fields would be able to determine the strength of the ISMRs. To this end, we investigate whether the monthly and seasonally mean wind features are distinct between strong and weak ISMs in section 3.2. We then proceed to examine the potential impacts of short-time fluctuations of surface wind fields on the rainfall over the four IMD regions and over the entire India (section 3.3 and 3.4). In section 3.5, we examine the northward propagation of surface wind fields from the BoB to Indian subcontinent, an important way ocean winds in the BoB contribute to the strength of ISMR.

3.1 Geographic distribution of monthly and seasonally mean rainfall in India during strong and weak ISMs

According to the definition of ISM strength discussed in section 2.1, we identify three strong ISM years (2005, 2007, and 2008) and three weak ISM years (2000, 2002, and 2009) during the period 1991–2014. Fig. 2 illustrates the geographical distribution of India's daily rainfall averaged over June, July, August, September (for individual months), and over JJAS (for the season as whole) during strong and weak ISMRs. Fig. 2 also shows the corresponding differences in rainfall geographic distribution between strong and weak ISMRs. A student-t two-sided test was conducted to determine whether these differences of daily rainfall averaged over June, July, August, September and JJAS between strong and weak ISMRs are significant assuming the daily rainfalls for strong and weak ISMRs have the same variance distribution. Only the significant differences at the 99% confidence level are shaded. It is clear that during June, rainfall does not appear significantly different between strong and weak ISMRs. However, during July, rainfall is significantly different over parts of SPIN and NWI. During August, the area of significant difference of rainfall in SPIN tends to be smaller and the rainfall does not appear significantly different in NWI. Interestingly, although most of the CI region gains more rainfall in July and August during strong ISMRs than during weak ISMRs, the rainfall difference in the CI region is overall insignificant. It is intriguing that the Western Ghats and the eastern portion of the SPIN between 15°N–20°N experience significantly larger rainfall during September of strong ISMs. Generally, the difference in rainfall over the NEI region is not significantly different, partly due to a large degree of uncertainty in relationship with the strength of ISMR (Zheng et al. 2016a, b). The phenomena described above can be partially explained by anomalous wind features on short timescales over the Indian Ocean during different ISM years, which are discussed in section 3.3–3.4.

3.2 Links of monthly and seasonally mean surface wind fields to ISMR strength

3.2.1 Surface wind vector

Fig. 3 is the same as Fig. 2 but shows surface wind vector over the Indian Ocean for strong and weak ISMs, and the corresponding differences. The general spatial patterns of monthly and seasonally mean wind vector are alike: the southeast winds over the southern Indian Ocean cross the equator and turn rightward to become southwest winds. Five regions—the AS (denoted by red rectangle box), the BoB (denoted by black rectangle box), the SIO (denoted by blue rectangle box), the SC (denoted by green rectangle box), and the EIO (denoted by cyan rectangle box)—were chosen because the temporally mean and variability of winds over these regions are postulated to play a role in rainfall strength in the Indian subcontinent. For example, winds along the SC and in the AS moving towards India may be essential to the transport of moisture to India, while energetic convective systems in the BoB may affect Indian rainfall. Wind variability in the EIO and the SIO may play a role in the phase shift of the IODs (i.e., shift among the positive, negative, and neutral phases of IODs) via atmosphere-ocean interaction, noting that the IOD itself is an important factor influencing the strength of ISMR (e.g., Ashok et al. 2001; Sreejith et al. 2015). Because surface wind features over the five major regions can affect ISMR, surface winds over the five regions are chosen for analysis and their possible links to the strength of ISMR are examined in this study.

Four striking features are found. First, monthly and seasonally mean winds are not significantly different over the BoB between strong and weak ISMRs, indicating that strength of seasonal and monthly mean winds over the BoB is not the significant factor in controlling the rainfall strength in India. Second, monthly mean winds over the AS are not significantly different, except in September when stronger winds over the AS towards the Indian subcontinent during strong ISMRs may result in the heavy rainfall in the regions along Western Ghats (as seen in Fig. 2n). The seasonal mean winds are also not significantly different over the AS. Third, a small portion of monthly mean winds along the SC is significantly different in June only, probably because the winds start turning over this region in this month. Fourth, winds are significantly different over some portion of the EIO only in June and August. Its association with Indian rainfall will be discussed in section 3.4.

3.2.2 Surface wind speed

Fig. 4 is the same as Fig. 3 but showing surface wind speed. In general, the spatial distributions of monthly and seasonal mean surface wind speed for different ISMs have several common features. For example, the surface wind speeds are the strongest along the SC and in the AS with a southwest tilt and the wind speeds in the BoB are much weaker than those in the AS. There is a zonal belt of strong wind speed in the SIO, especially during July and August. Regardless of these commonalities, there are also some features that are distinct between different strength of ISMs. For example, the surface wind speed over the AS in September of strong ISMs is significantly larger than during September of weak ISMs at a 99% confidence level. This partly explains the overall excessive rainfall over the western part of India in September of strong ISMs as compared to that during September of weak ISMs (as seen in Fig. 2n). In contrast, surface wind speeds are different in some portions of the EIO region between strong and weak ISMRs during June–August. It should be noted that the seasonal mean wind speeds in the BoB are not significantly different between strong and weak ISMRs. It is also worth noting that daily wind speed along SC (EIO) is well correlated with daily wind speed in the AS (SIO) and statistically correlated at a 99% confidence level during both strong and weak ISMs (not shown), indicating strong temporal synchronization for daily winds between SC and AS, as well as between EIO and SIO.

3.2.3 Surface wind convergence and curl

Surface wind convergence is an important process for drawing surface moisture up to the lower troposphere. Thus, the availability of a high-quality wind product with a high horizontal resolution allows us to examine the fine-scale features of wind convergence (Fig. 5). Both strong and weak ISMs share many common features with regards to surface wind convergence. First, surface divergence (convergence) is dominant in the interior of the AS (BoB) in the monsoon season except near the coastal area where the orographic effect causes strong surface convergence. Dominant surface divergence impedes the accumulation of surface moisture in the low-level atmosphere in the AS, which does not allow for the energy necessary to initiate and sustain the monsoon depressions, thus partly explaining the infrequent depressions (i.e., energetic convective activities) in the AS. By contrast, the dominant surface convergence in the BoB is accompanied by the presence of the positive wind curl/cyclonic vorticity. Second, the dominant surface convergence and actual high amount of moisture in the lower atmosphere above the SIO favor vertical transport of moisture from the surface to lower troposphere, This moisture is then transported towards the AS and BoB by southeasterly winds south of the equator and southwesterly winds north of the equator (see Fig. 3). The transported moisture above the AS converges along the Western Ghats and in monsoon trough region (mainly above the BoB), then produce rain through moist-thermodynamic processes. Conversely, moisture movement in the BoB toward the Indian subcontinent is not primarily achieved through mean winds; it is primarily through movement of a series of convective activities associated with monsoon low pressure system carrying abundant moisture toward the Indian subcontinent. When strong convective events make landfall, they produce heavy precipitation in the Indian subcontinent (Singh et al. 2001). Note that the dominant surface wind convergence in the BoB is usually produced by the monsoon trough in the BoB, which not only affects frequency and timing of convective events but also acts to direct convective events towards the Indian subcontinent. Thus, surface wind convergence in the BoB is an essential process to the initiation, development, and maintenance of the convective processes providing abundant moisture. As a consequence, when convective systems move toward the Indian subcontinent, the land receives heavy precipitation as moisture is condensed and latent heat is released to energize convective systems. Note that strong surface divergence along the SC during strong and weak ISMRs enhances the surface winds in the AS. Regardless of the important roles of surface wind convergence, the monthly and seasonal mean surface convergence in the SC, AS, BoB, and SIO during strong ISMRs are not significantly different from those during weak ISMRs. It is worth noting that surface convergence along the Western Ghats in September is remarkably different. This convergence results in a significant rainfall difference along the Western Ghats in September (Fig. 2n). Although the monthly and seasonal mean surface convergence are generally not significantly different between strong and weak ISMRs in the AS, BoB, and SIO, we postulate that it is the variability of surface wind convergence on short timescales (e.g., up to one week) in the above three regions that plays a critical role in the strength of ISMRs. This will be further investigated in section 3.4.2.

The features of monthly mean surface wind curl between strong and weak ISMRs (not shown) are similar to surface wind convergence (Fig. 5). This is not surprising because surface wind curl is strongly connected with wind convergence/divergence and cyclonic (anti-cyclonic) circulation induces cross-isobar flow in the boundary layer leading to surface convergence (divergence) caused by turbulent friction and Ekman transport.

3.3 Probability density function distribution based on daily surface wind fields

The results presented thus far clearly demonstrate that the monthly and seasonally mean wind fields in the three regions are overall not significantly different except over the AS in June and

September. Hence, it is natural to ask what causes significantly different ISMRs. Here, we propose that the wind variability on short timescales (e.g., up to one week) plays a more important role than the monthly and seasonal mean fields in the Indian summer monsoon rainfall, which further supports the notion that the interannual variability of ISMR is more dependent on the scales which are shorter than a month (Goswami and Xavier 2005; Webster et al. 1998) from the perspective of surface winds. This hypothesis is confirmed using high-quality CCMP wind products and the IMD's daily gridded rainfall product. In this section, the salient features regarding the PDF distributions of daily surface wind speed, convergence, and curl over the SC, AS, BoB, EIO, and SIO are examined for June, July, August, September, and for June–September. The PDF distributions are compared between strong and weak ISMRs. A PDF analysis based on the daily surface wind fields enables us to identify remarkable differences that are indistinguishable based on monthly mean fields (i.e., surface wind speed, convergence, and curl) in the five regions between strong and weak ISMRs by taking daily fluctuations into account.

3.3.1 Daily surface wind speed

The southwest wind speed in the AS is critically important for transporting moisture from the AS to India, thus affecting rainfall in India (Figs. 2–4). The PDF distribution of daily surface wind speed averaged over the AS (represented by a red rectangle in Fig. 4k) between different categories of ISMs is shown in Fig. 6. It is clear that the PDF distributions of daily wind speed averaged in the AS are distinguishable between each month of strong and weak ISMs, and these PDF distributions for strong and weak ISMRs are also different from normal ISMRs and all Indian summer monsoon periods, particularly in September. Interestingly, strong winds (> 10 m/s) are present more frequently during strong ISMRs than during weak ISMRs. This suggests that more frequent strong wind events on weather timescales tend to cause strong rainfall in India. The PDF distributions during normal ISMRs are expected to be comparable to those during the all ISMs since 75% (18 of 24) of the ISMRs are normal ISMRs. Interestingly, the PDF shape of each month is different from the other for normal and all ISMRs, implying that each month has its own salient wind speed features in the AS. During June of strong ISMRs, wind speeds have a wider range (4–13 m s^{-1}) than those (6.5–12 m s^{-1}) occurring during June of weak ISMRs, however, integration of the PDF distribution along x-axis turns out a similar time-mean value. Since surface wind speed in September is significantly distinguishable between strong and weak ISMs (see Fig. 4n), its significance can be explained by the PDF distribution—more (less) frequent strong wind events and less (more) frequent weak wind events during September of strong (weak) ISMs. Fig. 7 is the same as Fig. 6 except for winds along the SC. Results indicate that large daily winds along the SC occur more frequently during strong than weak ISMRs, similar to winds over the AS. However, some distinctions are also evident between strong and weak ISMRs, particularly in August, during which the range of daily wind speed along the SC (9–13 m s^{-1}) is narrower than the range of winds over the AS (6–12 m s^{-1}).

Similar to the PDF distribution in the AS, the PDF distribution of daily surface wind speeds in each month in the BoB also differs between strong and weak ISMRs, which is also different from that during normal ISMRs (not shown). The PDF distribution for daily surface wind speeds over the SIO (Fig. 8) is quite different from the distribution in the AS and BoB. First, daily wind speed in the SIO has a very narrow range (5–10 m s^{-1}) with a peak frequency of 7–8 m s^{-1}. Second, there is no significant difference between monsoon months. And finally, the slightly larger monthly mean wind speed in June and July over the SIO during strong ISMRs is primarily caused by the more frequent stronger winds. The PDF features for daily wind speed over the EIO between strong and weak ISMRs (not shown) are overall similar to those over the SIO except that wind speeds over the EIO have a strong frequency spectrum for low and high winds than those over the SIO. This happens probably because the variability of daily wind speeds over the EIO is stronger than that averaged over the entire SIO (not shown).

3.3.2 Daily surface wind convergence

The monthly area-averaged wind convergence (denoted by positive values) in the BoB is dominant during the entire summer monsoon seasons (Fig. 9), providing energy for the genesis, development, and maintenance of tropical convective systems in the BoB. Thus, the fluctuations of surface convergence field on weather timescales may be responsible for the extreme rainfall events on these timescales, leading to the remarkable difference in rainfall between strong and weak ISMRs as found by Zheng et al. (2016b). Since the monthly and seasonally mean convergence are overall not statistically different in all months (as seen in Fig. 5), it is likely that the number and strength of extremely stronger convergence events (> 6×10^{-6} s^{-1}) on short timescales (e.g., up to one week) during strong monsoons produce the differences in Indian rainfall. This indicates that the monthly and seasonally mean values alone are not sufficient to identify the potential links between surface wind convergence in the BoB and rainfall in India. Instead, the daily wind convergence variability in the BoB can be more relevant than its monthly and seasonally mean fields to the strength of ISMRs. This may help explain why rainfall in India adjacent to the BoB is statistically different during September between strong and weak ISMRs (Fig. 2n), while the convergence averaged in September is not statistically significantly different (Fig. 5n).

Unlike wind convergence over the BoB, the dominant surface wind convergence in the AS is primarily located in the regions adjacent to the western coast of the Indian subcontinent due to the orographic effects. Additionaly, the monthly mean wind convergence are overall not significantly different between strong and weak ISMRs (Fig. 5). However, similar to Fig. 9 for wind convergence over the BoB, the PDF distributions of the daily surface wind convergence area averaged over the AS are also distinct between strong and weak ISMRs in Jun and September (not shown). The distinctions in the PDF of daily wind convergence in June and September partly explain daily rainfall variations along the Western Ghats, underscoring the importance of daily fluctuation of wind convergence over the AS (particularly in the west coast regions) to bring heavy rainfall along the Western Ghats. In fact, a recent study (Varikoden et al. 2019) indicated rainfall patterns over the Western Ghats changed during the period 1931–2015: the average rainfall in the northern Western Ghats increased by 2% per decade while in the southern region it reduced by 3% per decade. The authors further suggested that the change in rainfall patterns in the Western Ghats is associated with a northerly shift of low level jetstream over the Arabian sea.

Similar to the narrow range for the PDF of daily wind speed in the SIO (Fig. 8), the PDF range of daily wind convergence over the SIO is also narrow ($0–2\times 10^{-6}$ s^{-1}), compared to those over the BoB (Fig. 9) and the convergence is dominant over entire summer monsoon season (not shown). It should be noted that the persistent existence of dominant surface wind convergence in the SIO is critically important for the lower troposphere in the tropics to obtain moisture from the underlying ocean surface. The accumulated moisture is transported to the AS and BoB, acting as important moisture sources for developing convective events/monsoon depressions in the BoB.

3.3.3 Daily surface wind curl

The energetics of monsoon depressions in the Indian Ocean can be represented by the variability of surface wind curl. While the monthly mean values (derived from daily wind curls) over the BoB are similar for strong and weak ISMRs, the PDF distribution for daily surface wind curl over the BoB is different in each month (Fig. 10). Regardless of similar monthly mean values, more extreme daily surface curls (> 4×10^{-6} s^{-1}) occur over the BoB during September of strong ISMRs, which partly explain the significantly more rainfall in east of the SPIN (Fig. 2n).

Similar to Fig. 10, the PDF analysis of daily surface wind curl over the AS between strong and weak monsoons illustrates the distinct features in surface wind curl on short timescales (not shown). The PDF distributions for daily surface wind curl and convergence over the EIO and SIO are alike for both strong and weak ISMRs (not shown). Although the PDF distributions of daily surface wind curl are distinct to some extent between strong and weak ISMRs, the monthly mean fields are similar. The PDF shape is also similar among months of normal ISMRs.

It is worth noting that the above changes in surface wind fields may be associated with the SST distribution, though SST is usually a slow varying variable on short timescales. Surface wind stress divergence along with SST is critical for air-sea interaction and the stability of the marine atmospheric boundary layer, which can cause a change in monsoonal circulation, ultimately giving rise to the rainfall variations in India.

The association of surface wind speed, convergence, and curl with regional rainfall on short timescales (e.g., weather scales) will be further discussed in the next section to prove our hypothesis that the short time fluctuations of wind fields play a more important role than monthly and seasonal mean wind fields in controlling the strength of ISMRs.

3.4 Lag correlation of daily surface wind speed, convergence, and curl with regional rainfall

The analysis in section 3.2 does not consider temporal variability of surface wind fields when discussing the association between surface winds and rainfall in India. By considering daily fluctuations (anomalies), this section presents the simple linear lag-lead correlation analysis between anomalies of daily surface wind fields (speed, convergence, and curl) and anomalies of daily rainfall in the four IMD rainfall zones to establish the basic relationship between Indian Ocean surface winds and regional rainfall in India on weather timescales.

3.4.1 Lag correlation between daily surface wind speed and daily regional rainfall

The relationships between daily surface wind speed over the SC, AS, BoB, EIO, and SIO and daily rainfall in the four IMD regions and the all-India rainfall are distinct for different categories of ISMRs (Fig. 11). First, the daily surface wind speed over the AS overall has the best correlation with daily rainfall over the entire Indian region except in NEI regardless of ISM strength. The lag/lead pattern of correlation for surface wind speed along the SC are overall akin to those over the AS except during strong ISM years when wind speed over the SC has long persistent lead time with rainfall in CI while the correlation of wind speed over the AS with rainfall in CI drops rapidly (i.e., correlation becomes insignificant when winds in the AS lead rainfall in CI more than seven days). Surface wind speed in the BoB is also highly correlated with rainfall in NWI, CI, and SPIN regardless of ISM strength. Surface wind speed in the EIO and SIO is generally poorly correlated with rainfall in the four regions on weather timescales. It should be noted that daily surface wind speed in the AS is better correlated with daily rainfall in NWI and CI during strong ISMRs than during normal and weak ISMRs. Second, rainfall in NEI is generally poorly correlated with surface wind speed in the AS, BoB, and SIO, implying that the controlling mechanisms for rainfall in NEI differ from the other three homogeneous rainfall zones of India. We postulate that NEI rainfall is likely affected by the variability of the East Asian monsoons and/or monsoons over western north Pacific regions via westward propagation of 10–20-day mode from the western Pacific (Krishnamurti and Ardunay 1980; Chen and Chen 1993; Chatterjee and Goswami 2004; Fukutomi and Yasunari 1999; Annamalai and Slingo 2001). Third, surface wind speeds in the AS and BoB generally lead rainfall in NWI and CI by several days (from one day to one week; i.e., on weather timescales) during strong, weak, and normal ISM years. The high correlation between surface wind speed in the AS and rainfall in NWI and CI is primarily because the prevailing surface wind direction in the AS is directly toward the Indian subcontinent, efficiently bringing abundant moisture to India. The high correlation between surface wind speed in the BoB and Indian rainfall can be misleading without support of physical processes because the prevailing mean surface wind direction in the BoB is almost parallel to the east coast of India and may be only a continuation of airstream from the AS to BoB. However, the surface wind convergence in the BoB is one of the most critical processes for rainfall in India compared to that in the AS and SIO, as discussed in the following subsection.

3.4.2 Lag correlation between daily surface wind convergence/curl and regional rainfall

Moisture convergence via surface wind convergence in the Indian Ocean is one of the most important processes for the development and maintenance of convective systems in the Indian Ocean. When these systems move toward the Indian subcontinent, they greatly influence the inland rainfall. Fig. 12 presents the lag-lead correlation between the daily surface wind convergence and the regional and total rainfall in India during strong, normal, and weak ISM years. The simple linear relationship shows the distinct roles of daily fluctuation of surface wind convergence over the SC, AS, BoB, EIO, and SIO in rainfall over the different IMD regions during strong, normal, and weak ISM years. Surface wind convergence in the BoB is overall best correlated with all-India rainfall with a lead of 1–10 days, probably because the number and intensity of monsoon depressions associated with surface convergence in the BoB prevail compared to other ocean regions or because a part of the monsoon trough is usually located in the BoB. Thus, the surface convergence over the BoB has a predictive value of a few days for all-India rainfall. Such correlation in the BoB during strong ISM years is better than normal and weak ISM years, particularly with rain in CI. This happens because monsoon low pressure and convective systems affecting Indian rainfall are more robust during strong ISM years and less energetic during the weak ISM years (Goswami et al. 2003) as well as normal ISM years. In addition, a strong (weak) ISMR generally has strong (weak) "active" phases and weak (strong) "break" phases of monsoons (Zheng et al. 2016b). Interestingly, compared to other three IMD regions, surface wind convergence in the BoB is strongly and negatively correlated with rainfall in NEI with a lead of 0–2-days. Wind convergence along the SC and in the AS is poorly correlated with Indian rainfall on short timescales.

In addition, the surface wind convergence in the EIO and SIO is poorly correlated with Indian rainfall on weather timescales during strong, normal, and weak ISM years, except in CI during strong ISM years where negative correlation dominates. Such negative correlation may be associated with the enhanced surface wind divergence over the SIO as a part of downwelling branch of Hadley circulation during strong ISMRs when meridional monsoonal circulation (i.e., Hadley circulation) strengthens. It is also clear that the correlations during normal ISMRs are overall the weakest relative to those during strong and weak ISMRs. We hypothesize that anomalous surface wind features in the EIO and SIO may affect Indian rainfall on longer timescales rather than at short timescales (e.g., weather timescales) in several ways.

The relationships between wind curl and regional rainfall (not shown) are similar to those between wind convergence and regional rainfall as shown in Fig. 12. For example, surface wind curl in the BoB during strong ISMRs has the best correlation with rainfall in SPIN, CI, NWI with dominant leading days of 2, 6–9, and 10, respectively. Wind curl in the AS and SC is overall poorly correlated with Indian rainfall. It should be pointed out that the correlation between surface wind curl and rainfall in NEI is generally not significant, which is consistent with Zheng et al. (2016b) who found that rainfall in NEI is not primarily determined by the robustness of convective system in the BoB. A recent study (Choudhury et al. 2019) suggested that the decreasing trend of ISMR in NEI during 1979–2014 can be associated with the strong interdecadal variability of the subtropical Pacific Ocean. Table 1 summarize the lead-lag correlations between the daily rainfall over the four IMD regions (and over all India) and the daily fluctuation of wind fields in the three Indian Ocean regions.

3.5 Northward propagation of surface wind fields over the BoB

Correlation analyses in section 3.4.2 clearly show that the surface wind convergence and curl over the BoB affect the rainfall in India on synoptic timescales. This section provides observational evidence that surface winds over the BoB affect rainfall in India through the northward propagation of surface wind curl and convergence from ocean to land. It is well known that ISMR exhibits prominent intraseasonal variations across a wide spectrum of timescales, mostly on the timescales of 30–60 days and 10–20 days. The 30–60-day mode is represented by a large horizontal scale northward propagation at approximately 1–2 m s^{-1} and eastward propagation speed of about 6 m s^{-1} that moves from Indian Ocean toward South Asia and East Asia (Kikuchi et al. 2012) and the 10–20-day mode is represented by the westward propagation that moves from the western Pacific to about 70°E with a phase speed of about 4.5 m s^{-1} (Krishnamurti and Ardunary 1980; Chen and Chen 1993; Chatterjee and Goswami 2004). The two modes are usually captured by daily outgoing longwave radiation (OLR) and rainfall (Kikuchi et al. 2012). In fact, the northward propagation is also captured by daily surface wind curl over the BoB during strong and weak ISMRs (Fig. 13). The northward propagating signal is clearly seen during the entire monsoon seasons of both strong and weak ISMRs, during which the largest wind curl is found to propagate northwestward during September 2005 and Jun 2007. The northward propagating signal can move either eastward or westward, with a slow westward propagation and a fast eastward propagation. Such features are likely associated with the different phase speeds of dominant modes at intraseasonal (a fast eastward propagating 30–60-day mode) and synoptic (a slow westward propagating 10–20-day mode) scales. It should be noted that the surface wind convergence fields have the similar features (not shown). The above results indicate the prevalent northwestward on intraseasonal timescales and northeastward propagation modes on synoptic timescales captured by convective bands are also well captured by the surface wind fields.

4 Discussion

An MLR approach is used to estimate the anomalous monthly rainfall in India from anomalous monthly wind fields and examine the relative roles of monthly wind fields over the AS, BoB, and SIO in the total Indian rainfall and in the four IMD regions during Indian summer monsoons. We exclude the SC and EIO for MLR analysis because monthly mean wind variability over the SC (EIO) is similar to that over the AS (SIO) (not shown) and surface winds in the AS, BoB, and SIO can represent winds in most of Indian Ocean adjacent to Indian subcontinent that are closely associated with ISMR. Tables 2–6 summarize the MLR results. Tables 2 and 3 indicate that monthly wind speed in the AS and BoB is important to the monthly rainfall in all India and NWI. Table 4 shows that the monthly wind speed in the AS can significantly affect monthly rainfall in CI. Table 5 suggests that monthly wind speed in the BoB and monthly wind convergence in the AS and BoB can significantly affect monthly rainfall in SPIN, and Table 6 reveals that monthly wind fields (speed, convergence, and curl) in the AS, BoB, and SIO do not significantly control the monthly rainfall in NEI. These results suggest that the fluctuations of monthly wind fields in the AS, BoB can affect monthly rainfall in some regions (e.g., in NWI, CI, and SPIN). It should be noted that the fluctuations of monthly wind fields cannot cause a significant change of rainfall over the entire India because the differences in monthly mean wind fields are overall insignificant between strong and weak ISMRs (Figs. 3–5). The results from the five tables imply that the controlling mechanisms by monthly wind fields over Indian Ocean for monthly rainfall in NWI, CI, and SPIN are similar to some degree, but distinct from those for rainfall in NEI, which may be more associated with wind features over the western Pacific.

Furthermore, we are able to estimate the monthly rainfall in the entire India from the monthly surface wind fields over the AS, BoB, and SIO using an MLR approach. Fig. 14 shows the time series of the anomalous monthly rainfall (June–September; red curve) estimated from the total and individual components using the MLR model (i.e., Eq. 1) and compared to the actual anomalous monthly rainfall (June–September; black curve) computed from the daily gridded rainfall during the 24 Indian summer monsoon seasons (i.e., 1991–2014). Fig. 14a compares the anomalous monthly Indian rainfall (June–September) with the rainfall estimated from the nine components using MLR. The anomalous monthly rainfall is closely tied to wind fields with the R^2 of 0.31, indicating 31% of the variance of monthly Indian rainfall is explained by the monthly wind fields in three regions (i.e., nine components: X_1 to X_9 in Eq. 1). Furthermore, the extremely large (small) rainfalls in some years (e.g., 2005 and 2009) do not necessarily imply the advent of extreme wind fields in the Indian Ocean.

The monthly mean surface wind speeds over the AS in summer months are significantly correlated with the monthly mean rainfalls (the correlation coefficient is 0.36) at the 99% confidence level, which makes the greatest contribution to the variations of monthly rainfall (with the largest linear regression coefficient 1.26, which is significant at the 99% level; see Fig. 14b and Table 2). Monthly wind speed over the BoB is poorly correlated with the monthly rainfall (Fig 14c), although the regression coefficient is significant at the 99% level (Table 2). Variations of monthly wind speed over the SIO cannot induce the variations of monthly Indian rainfall (Fig. 14d). Wind convergence over the AS is significantly correlated with monthly Indian rainfall (Fig. 14e), but has less influence (smaller and insignificant regression coefficient) relative to the wind speed over the AS. However, the change in monthly wind convergence over the BoB (Fig. 14f) is of secondary importance to the variations of monthly rainfall (with the second largest regression coefficient of 1.03 and significant at the 95% level, though not significant at the 99% level; Table 2). Monthly wind convergence over the SIO has no correlation with monthly Indian rainfall (Fig. 14g) and the regression coefficient is even insignificant at the 95% level. The insignificant regression coefficient and poor linear correlation between monthly mean wind curls over the BoB (SIO) and monthly Indian rainfall suggest that monthly mean wind curl plays an unimportant role in the strength of monthly Indian rainfall (Fig. 14i–j). Monthly wind curl over the AS is significantly correlated with monthly rainfall, but with a small regression coefficient. Note that surface wind convergence over the AS (Fig. 14e) has a similar correlation and a moderate regression coefficient (0.6) and because the surface wind convergence and surface wind curl are not interdependent: surface wind curl leads to the variations of surface wind convergence in the atmospheric boundary (i.e., surface cyclonic curl induces surface convergence and surface anti-cyclonic curl induces surface divergence), surface wind curl in the AS may play an indirect role in Indian rainfall through inducing variations of surface wind convergence in the AS. Root-mean-square error analysis indicates the monthly rainfall estimated from monthly wind speed and convergence over AS has the least root-mean-square error relative to the actual monthly Indian rainfall, in addition to their best correlation with the total rainfall. In summary, the monthly surface wind speed in the AS and the monthly wind convergence in the BoB play a dominant role in the variations of monthly rainfall, indicating that monthly surface winds in the AS and BoB may influence the monthly rainfall in different ways: monthly surface winds in the AS affect monthly rainfall in India by transporting moisture to India (i.e., surface wind speed matters) and monthly surface winds in the BoB influence monthly rainfall through convection processes charged by the surface moisture convergence (i.e., surface wind convergence matters). The above hypothesis will be tested in future work using the moisture datasets.

The above results also indicate that the strength of monthly wind fields is not the dominating factor in relation to extreme ISMRs. For example, exceptionally weak monthly mean winds are not found during the 2009 extremely weak ISMR period relative to other weak and strong ISMR periods (Fig. 14a).

5 Conclusions

Using the CCMP wind products and the IMD's daily gridded rainfall over the period 1991–2014, this study provides statistical evidence that short-time (i.e., sub-monthly) fluctuations of Indian Ocean surface winds are more related to the strength of ISMR than its long-time (i.e., monthly) fluctuations. Our results suggest that sub-monthly surface wind features could be useful in diagnosing rainfall characteristics. Two hypothetical baseline mechanisms on how short-time fluctuations of surface winds in the Indian Ocean may affect ISMR during strong and weak ISMRs are: (1) winds in the AS region affect ISMR through moisture transport by more frequent strong winds (wind speed) on short timescales during strong ISMRs than weak ISMRs, and (2) winds in the BoB affect ISMR through the northward movement of more frequent convective systems represented by more frequent surface wind curl (vorticity) and convergence in the BoB during strong ISMRs than weak ISMRs. The two hypotheses need validation in a future study.

There are some important caveats worth mentioning. In this study, only three strong and three weak ISMRs are available for analysis due to the short record of CCMP wind vector analysis product. This may not well represent the strong and weak ISMRs thus we caution readers that the results come from a relatively small number of samples. However, the features in rainfall and wind fields are well consistent with each other and the results shown in this study are supported in a physical sense, reinforcing our confidence that the results from this study are reliable to some degree.

Acknowledgments

We are grateful to the India Meteorological Department that provides the latest daily gridded rainfall data. We also greatly appreciate Remote Sensing Systems (RSS) for providing the Cross-Calibrated Multi-Platform (CCMP) Version 2.0 vector wind product. Data are available at www.remss.com. The Center for Ocean-Atmospheric Prediction Studies (COAPS) at the Florida State University provides computational facilities for this study. The study is fully supported by the National Aeronautics and Space Administration (NASA) Physical Oceanography in support of the Ocean Vector Winds Science Team (OVWST), NASA NEWS, and the NOAA Climate Observing Division (COD). We thank four anonymous reviewers for their insightful comments leading to the improvement of manuscript.

References

Ailikun B, Yasunari T (1998) On the two indices of Asian summer monsoon variability and their implications. *Extended Abstracts, Int. Conf. on Monsoon and Hydrologic Cycle*, Kyongju, Korea, Korean Meteorological Society, 222–224.

Allaby M (2002) Encyclopedia of Weather and Climate, Facts on Files Publishing. pp. 373. ISBN 0816040710, 9780816040711

Annamalai, H, Slingo JM (2001) Active/break cycles: Diagnosis of the intraseasonal variability of the Asian summer monsoon. Clim Dyn 18: 85–102.

Ashok K, Guan Z, Yamagata T (2001) Impact of the Indian Ocean Dipole on the relationship between the Indian monsoon rainfall and ENSO. Geophys Res Lett 28(23): 4499–4502. doi: 10.1029/2001GL013294

Atlas R, Hoffman RN, Ardizzone J, Leidner SM, Jusem JC, Smith DK, Gombos D (2011) A cross-calibrated, multiplatform ocean surface wind velocity product for meteorological and oceanographic applications. Bull Am Meteorol Soc 92: 157–174. doi: 10.1175/2010BAMS2946.1

Atlas R, Hoffman RN, Bloom SC, Jusem JC, Ardizzone J (1996) A multiyear global surface wind velocity dataset using SSM/I wind observations. Bull Am Meteorol Soc 77: 869-882

Bhanu Kumar OSRU (1988) Eurasian snow cover and seasonal forecast of Indian summer monsoon rainfall. Hydrological Sciences Journal 33(5): 515–525, doi: 10.1080/02626668809491278

Blanford HF (1884) On the connection of Himalayan snowfall with dry winds and seasons of drought in India. Proc Roy Soc, London, 37: 3–22.

Cadet DL, Greco S (1987a) Water vapor transport over the Indian Ocean during the 1979 summer monsoon Part 1: Water vapour fluxes. Mon Wea Rev 115: 653–663

Cadet DL, Greco S (1987b) Water vapor transport over the Indian Ocean during the 1979 summer monsoon Part 2: Water vapor budgets. Mon Wea Rev 115: 2358–2366

Charney JG, Shukla J (1981) Predictability of monsoons. Monsoon Dynamics. Sir J. Lighthill and R. P. Pearce, Eds., Cambridge University Press, 99–109.

Chatterjee P, Goswami BN (2004) Structure, genesis and scale selection of the tropical quasi-biweekly mode. Quart J Roy Meteorol Soc 130: 1171–1194.

Chen, TC, Chen JM (1993) The 10 to 20-day mode of the 1979 Indian monsoon: Its relation with the time variation of monsoon rainfall. Mon Wea Rev 121: 2465–2482.

Choudhury, BA, Saha SK, Konwar M, Sujith K, Deshamukhya A (2019) Rapid drying of Northeast India in the last three decades: Climate change or natural variability? J Geophys Res, 124: 227–237. https://doi.org/10.1029/2018JD029625

Dey B, Bhanu Kumar OSRU (1982) An apparent relationship between Eurasian snow cover and the advanced period of the Indian summer monsoon. J Appl Meteor 21: 1929–1932.

Dey B, Bhanu Kumar OSRU (1983) Himalayan winter snow cover area and summer monsoon rainfall over India. J Geophys Res 88: 5471–5474

Dickson RR (1984) Eurasian snow cover versus Indian monsoon rainfall – An extension of the Hahn-Shukla results. J Climate Appl. Meteor. 171–173.

Findlater J (1969) A major low-level air current near the Indian Ocean during the northern summer. Quart J Roy Meteorol Soc 95: 362–380, https://doi.org/10.1002/qj.49709540409

Fukutomi Y, Yasunari T (1999) 10–25 day intraseasonal variations of convection and circulation over east Asia and western north Pacific during early summer. J. Metorol Soc. Japan 77(3): 753–769.

Goswami BN, Ajayamohan RS, Xavier PK, Sengupta D (2003) Clustering of synoptic activity by Indian summer monsoon intraseasonal oscillations. Geophys Res Lett 30: 1431. doi: 10.1029/2002GL016734

Goswami BN, Krishnarmurthy V, Annamalai H (1999) A broad scale circulation index for the interannual variability of the Indian summer monsoon. Quart J Roy Meteor Soc 125: 611–633.

Goswami BN, Xavier PK (2005) ENSO control on the south Asian monsoon through the length of the rainy season. Geophys Res Lett 32, L18717, doi: 10.1029/2005GL023216

Govardhan D, Rao VB, Ashok K (2017) Understanding the revival of the Indian summer monsoon after breaks. J Atmos Sci, 74: 1417–1429, doi: 10.1175/JAS-D-16-0325.1

Hahn DJ, Shukla J (1976) An apparent relationship between Eurasian snow cover and Indian monsoon rainfall. J Atmos Sci 33: 2461–2462.

Hoffman RN, Leidner M, Henderson JM, Atlas R, Ardizzone JV, Bloom SC (2003) A two-dimensional variational analysis method for NSCAT ambiguity removal: methodology, sensitivity, and tuning. J Atmos Oceanic Technol 20: 585-605

Joseph PV, Mukhopadhyaya RK, Dixit WV, Vaidya DV (1981) Meridional wind index for long range forecasting of Indian summer monsoon rainfall. Mausam, 32: 31–34.

Kikuchi K, Wang B, Kajikawa Y (2012) Bimodal representation of the tropical intraseasonal oscillation. Clim Dyn 38: 1989 – 2000, doi: 10.1007/s00382-011-1159-1.

Konwar M, Parekh A, Goswami BN (2012) Dynamics of east-west asymmetry of Indian summer monsoon rainfall trends in recent decades. Geophys Res Lett 39, L10708, doi: 10.1029/2012GL052018.

Krishnamurti, TN, Ardunay P (1980) The 10 to 20 day westward propagating mode and breaks in the monsoons. *Tellus* **32**: 15–26.

Krishnamurthy L, Krishnumurthy V (2014) Influence of PDO on south Asian summer monsoon and monsoon-ENSO relation, Clim Dyn 42:2397–2410, doi: 10.1007/s00382-013-1856-z

Krishnamurthy V, Shukla J (2000) Intraseasonal and interannual variability of rainfall over India. J Clim 13: 4366–4377.

Krishnan R, Swapna P (2009) Significant influence of the boreal summer monsoon flow on the Indian Ocean response during dipole events. J Clim 22: 5611–5634, doi: 10.1175/2009jCLI2176.1

Kulkarni A, Sabade SS, Kripalani RH (2006) Intra-seasonal vagaries of the Indian summer monsoon rainfall. Indian Institute of Tropical Meteorology, ISSN 0252-1075, Research Report No. RR-114

Lau KM, Chan PH (1986) Aspects of the 40 – 50 day oscillation during the northern summer as inferred from ongoing longwave radiation. Mon Wea Rev 114: 1354–1367.

Levine RC, Turner AG (2012) Dependence of Indian monsoon rainfall on moisture fluxes across the Arabian Sea and the impact of coupled model sea surface temperature biases. Clim Dyn 38: 2167–2190

Li J, Zeng Q (2002) A unified monsoon index. Geophys Res Lett 29(8): 1274, doi: 10.1029/2001GL013874

Malik A, Brönnimann S (2018) Factors affecting the inter-annual to centennial timescales variability of Indian summer monsoon rainfall. Clim Dyn 50: 4347–4364, doi: 10.1007/s00382-017-3879-3

Malik A, Brönnimann S, Stickler A, Raible CC, Muthers S, Anet J, Rozanov E, Schmutz W (2017) Decadal to multi-decadal scale variability of Indian summer monsoon rainfall in the coupled ocean-atmosphere-chemistry climate model SOCOL-MPIOM. Clim Dyn 49: 3551–3572, doi: 10.1007/s00382-017-3529-9

Pai DS, Sridhar L, Kumar R (2016) Active and break events of Indian summer monsoon during 1901–2014. Clim Dyn 46: 3921–3939. doi:10.1007/s00382-015-2813-9

Parthasarathy B, Kumar KR, Deshpande VR (1991) Indian summer monsoon rainfall and 200-mbar meridional wind index: application for long-range prediction. Int J Climatology 11: 165 – 176, doi: 10.1002/joc.3370110205

Parthasarathy B, Kumar RR, Kothawale DR (1992) Indian summer monsoon rainfall indices, 1871–1990. Meteor Mag 121: 174–186.

Parthasarathy B, Sontakke NA, Munot AA, Kothawale DR (1990) Vagaries of Indian monsoon rainfall and its relationship with regional/global circulations. Mausam 41: 301–308

Pattanaik DR (2007a) Analysis of rainfall over different homogeneous regions of India in relation to variability in westward movement frequency of monsoon depressions. Nat Hazards 40: 635–646

Pattanaik DR (2007b) Variability of convective activity over the northern Indian Ocean and its association with monsoon rainfall over India. Pure Appl Geophys 164: 1527–1545

Rao Y (1976) Southwest monsoon; meteorological monograph, synoptic meteorology, No 1/1976, India Meteorological Department.

Sadhuram Y, Ramesh Kumar MR (1988) Does evaporation over the Arabian Sea play a crucial role in moisture transport across the west coast of India during an active monsoon period? Mon Wea Rev 116: 307–312

Saha SK, Hazra A, Pokhrel S, Chadhari HS, Sujith K, Rai A, Rahaman H, Goswami BN (2019) Unraveling the mystery of Indian summer monsoon prediction: Improved estimate of predictability limit. J Geophys Res 124: 1962–1974, https://doi.org/10.1029/2018JD030082

Sikka DR, Gadgil S (1980) On the maximum cloud zone and the ITCZ over India longitude during the southwest monsoon. Mon Wea Rev 108: 1840–1853.

Skula J (1987) Interannual variability of monsoons. Monsoons, Fein and Stephens, Eds., A Wiley-Interscience, 399–464.

Singh OP, Ali Khan TM, Rahman DdS (2001) Has the frequency of intense tropical cyclones increased in the north Indian Ocean? Current Science 80(4): 575–580

Sreejith OP, Panickal S, Pai S, Rajeevan M (2015) An Indian Ocean precursor for Indian summer monsoon rainfall variability. Geophys Res Lett 42: 9345–9354. doi: 10.1002/2015GL065950

Varikoden H, Revadekar JV, Kuttippurath J, Babu CA (2019) Contrasting trends in southwest monsoon rainfall over the Western Ghats region of India. Clim Dyn 52: 4557–4566, https://doi.org/10.1007/s00382-018-4397-7

Venugopal T, Ali MM, Bourassa MA, Zheng Y, Goni GJ, Foltz GR, Rajeevan M (2018) Statistical evidence for the role of southwestern Indian Ocean heat content in the Indian summer monsoon rainfall, Scientific Reports, 8:12092, doi: 10.1038/s41598-018-30552-0

Verma RK, Kmate PP (1980) Statistical technique for long-range forecasting of summer monsoon activity over India. *Proceeding of Symposium on The Probabilistic and Statistical Methods in*

Weather Forecastings, 8–12 September 1980, Nice, World Meteorological Organization, Geneva, pp. 303–307.

Vernekar AD, Zhou J, Shukla J (1995) The effect of Eurasian snow cover on the Indian Monsoon. J Clim 8: 248–266.

Walker GT (1910) On the meteorological evidence for supposed changes of climate in India. Mem Indian Meteor, 21: 1–21.

Wang B, Fan Z (1999) Choice of south Asian summer monsoon indices. Bull Amer Meteor Soc 80: 629–638.

Webster PJ, Magana VO, Palmer TN, Shukla J, Tomas RT, Yanai M, Yasunari T (1998) Monsoons: Processes, predictability and the prospects of predictions. J Geophys Res 103: 14,451–14,510.

Webster P, Yang S (1999) Monsoon and ENSO: Selectively interactive systems. Quart J Roy Meteor Soc 118: 877–926.

Yusunari T (1979) Cloudiness fluctuation associated with the norther hemisphere summer monsoon. J Meteorol Soc Japan 57: 227–242.

Zheng Y, Ali MM, Bourassa MA (2016a) Contribution of monthly and regional rainfall to the strength of Indian summer monsoon. Mon Wea Rev 144: 3037–3055. doi:10.1175/MWR-D-15-0318.1

Zheng Y, Bourassa MA, Ali MM, Krishnamurti TN (2016b) Distinctive features of rainfall over the Indian homogeneous rainfall regions between strong and weak Indian summer monsoons. J Geophys Res Atmos 121 doi:10.1002/2016JD025135

Figure Captions

Fig. 1 Evolution of JJAS Indian rainfall (in mm) area-averaged over (a) all India, (b) NWI, (c) CI, (d) SPIN, and (e) NEI during the period 1991–2014 derived from the daily gridded (1°×1°) rainfall product provided by IMD. The JJAS rainfall averaged over all India and the four IMD regions during strong, weak, and normal monsoon years is denoted in blue, red, and gray, respectively. Strong, weak, and normal ISMRs are identified by the departure of JJAS rainfall area-averaged over all India each year from the JJAS rainfall climatology computed (i.e., 938 mm) computed from the daily gridded rainfall over the period 1951–2014, whose departure values are larger than +10%, smaller than –10%, and within –10% and +10% of the seasonally climatology, respectively. The blue (red) dashed line denotes a value of 110% (90%) of seasonal climatology (i.e., the mean climatology is 938 mm), which is 1031 mm (844 mm). The years of strong and weak ISMRs are denoted by the numbers over the bars in panel (a).

Fig. 2 Geographic distribution of monthly and seasonally averaged rainfall derived from daily rainfall (in mm) during strong and weak ISMRs as well as their corresponding differences (rainfall during strong ISMR years minus rainfall during weak ISMR years) between strong and weak ISMR years. The statistically significant differences at the 99% confidence level are shaded. The left (right) color bar is for time mean (difference) values.

Fig. 3 Same as Fig. 2 except for surface wind vector in the Indian Ocean. AS (57°E–72°E, 10°N–22°N), BoB (83°E–95°E, 10°N–18°N), SC (50°E–55°E, 5°N–10°N), EIO (80°E–100°E, 15°S–0°N), and SIO (50°E–100°E, 15°S–0°N) are delimited by a black, red, green, cyan, and blue rectangle, respectively. Unit: m s^{-1}.

Fig. 4 Same as Fig. 3 except for surface wind speed. The left (right) color bar is for temporal mean (difference) values. Unit: m s^{-1}.

Fig. 5 Same as Fig. 4 except for surface wind convergence. Positive (negative) value on the left two panes denotes surface convergence (divergence). The left (right) color bar is for temporal mean (difference) values. Unit: 10^{-6} s^{-1}.

Fig. 6 PDF distribution of daily surface wind speed over the Arabian Sea during strong, weak, normal ISMR years, and across all years (1991–2014). All counts are normalized to 100 for comparison purposes among the months of each ISMR category, so that the integration of the y values over the axis represents the occurring probability (in %) for each surface wind range.

Fig. 7 Same as Fig. 6 except for daily surface wind speed along the Somali coast (SC).

Fig. 8 Same as Fig. 6 except for daily surface wind speed over the Southern Indian Ocean.

Fig. 9 Same as Fig. 8 except for daily surface wind convergence over the Bay of Bengal.

Fig. 10 Same as Fig. 9 except for daily surface wind curl over the Bay of Bengal.

Fig. 11 Lag correlation between daily surface wind speed over the AS, BoB, SIO, SC, EIO and daily rainfall over (a) NWI, (b) CI, (c) SPIN, (d) NEI, (e) all-India during strong ISM years. (f)–(j) and (k)–(o) is the same as (a)–(e) but for normal and weak ISM years, respectively. "+" ("–") days in x-axis denote surface wind speed leads (lags) rainfall.

Fig. 12 Same as Fig. 11 except for lag correlation between daily surface wind convergence and daily rainfall.

Fig. 13 Time-latitude plot of the daily surface wind curl ($\times 10^{-6}$ s^{-1}) averaged between 83°E and 95°E (top panel in every year) and time-longitude plot of the daily surface wind curl averaged between 5°N and 10°N (bottom panel in every year) over the Bay of Bengal during strong (left) and weak (right) ISMRs. Plots show only positive values of surface wind curl (representing cyclonic vorticity).

Fig. 14 Anomalous monthly rainfall (in red) in June through September estimated from wind speed, wind convergence, and wind curl in the AS, BoB, and SIO using multiple linear regression model was compared to the actual rainfall (in black). (a) Rainfall estimated from the total nine components; (b) (c), (d) Rainfall estimated from wind speed in the AS, BoB, and SIO, respectively; (e), (f), (g) Rainfall estimated from wind convergence in the AS, BoB, and SIO, respectively; and (h), (i), (j) Rainfall estimated from wind curl in the AS, BoB, and SIO, respectively. Correlation coefficient and root-mean-square error (rmse) for each component are denoted at the left bottom of each panel.

Table Captions

Table 1 Summary of lead-lag correlations between daily rainfall over the four IMD regions and over all-India and daily fluctuation of wind fields (i.e., wind speed (wspd), wind convergence (conv), and win curl (curl)) in the three Indian Ocean regions (i.e., AS, BoB, SIO) for strong and weak ISMRs. Whether the correlation of wind fields leading rainfall up to one week is significant at a 99% confidence level is denoted by “Yes” or “No”.

		AS			BoB			SIO		
		wspd	conv	curl	wspd	conv	curl	wspd	conv	curl
Strong ISMRs	NWI	Yes	No	No	Yes	Yes	Yes	No	No	No
	CI	Yes	Yes	No	Yes	Yes	Yes	No	No	No
	SPIN	Yes	No	No	Yes	Yes	Yes	No	No	No
	NEI	Yes	No	Yes	No	No	No	No	No	No
	all-India	Yes	No	No	Yes	Yes	Yes	No	No	No
Weak ISMRs	NWI	Yes	No	No	Yes	Yes	No	No	No	No
	CI	Yes	Yes	Yes	Yes	Yes	Yes	No	No	Yes
	SPIN	Yes	Yes	Yes	Yes	Yes	Yes	No	No	Yes
	NEI	Yes	No	No	No	Yes	Yes	No	No	Yes
	all-India	Yes	Yes	No	Yes	Yes	Yes	No	No	Yes

Table 2 Summary of multiple linear regression for anomalous monthly Indian rainfall and anomalous monthly wind fields in three ocean regions ($R^2 = 0.31$).

Components	Coefficients	Significance at 95% level	Significance at 99% level
Wind speed in AS (X_1)	1.26	Yes	Yes
Wind speed in BoB (X_2)	-0.85	Yes	Yes
Wind speed in SIO (X_3)	0.29	No	No
Wind conv in AS (X_4)	0.60	No	No
Wind conv in BoB (X_5)	1.03	Yes	No
Wind conv in SIO (X_6)	0.90	No	No
Wind curl in AS (X_7)	0.01	No	No
Wind curl in BoB (X_8)	-0.33	No	No
Wind curl over SIO (X_9)	0.23	No	No

Table 3 Summary of multiple linear regression for anomalous monthly Indian rainfall in NWI and anomalous monthly wind fields in three ocean regions ($R^2 = 0.21$)

Components	Coefficients	Significance at 95% level	Significance at 99% level
Wind speed in AS (X_1)	1.36	Yes	Yes
Wind speed in BoB (X_2)	-1.17	Yes	Yes
Wind speed in SIO (X_3)	0.35	No	No
Wind conv in AS (X_4)	0.17	No	No
Wind conv in BoB (X_5)	0.71	No	No
Wind conv in SIO (X_6)	0.34	No	No
Wind curl in AS (X_7)	0.13	No	No
Wind curl in BoB (X_8)	-0.27	No	No
Wind curl in SIO (X_9)	0.11	No	No

Table 4 Summary of multiple linear regression for anomalous monthly Indian rainfall in CI and anomalous monthly wind fields in three ocean regions ($R^2 = 0.38$)

Components	Coefficients	Significance at 95% level	Significance at 99% level
Wind speed in AS (X_1)	2.04	Yes	Yes
Wind speed in BoB (X_2)	-0.61	No	No
Wind speed in SIO (X_3)	0.65	No	No
Wind conv in AS (X_4)	1.55	No	No
Wind conv in BoB (X_5)	1.21	No	No
Wind conv in SIO (X_6)	1.62	No	No
Wind curl in AS (X_7)	-0.11	No	No
Wind curl in BoB (X_8)	-0.30	No	No
Wind curl in SIO (X_9)	0.46	No	No

Table 5 Summary of multiple linear regression for anomalous monthly Indian rainfall in SPIN and anomalous monthly wind fields in three ocean regions ($R^2 = 0.18$)

Components	Coefficients	Significance at 95% level	Significance at 99% level
Wind speed in AS (X_1)	0.998	No	No
Wind speed in BoB (X_2)	-1.20	Yes	No
Wind speed in SIO (X_3)	0.12	No	No
Wind conv in AS (X_4)	1.65	Yes	No
Wind conv in BoB (X_5)	2.06	Yes	No
Wind conv in SIO (X_6)	0.54	No	No
Wind curl in AS (X_7)	-0.62	No	No
Wind curl in BoB (X_8)	-0.44	No	No
Wind curl in SIO (X_9)	-0.08	No	No

Table 6 Summary of multiple linear regression for anomalous monthly Indian rainfall in NEI and anomalous monthly wind fields in three ocean regions ($R^2 = 0.10$)

Components	Coefficients	Significance at 95% level	Significance at 99% level
Wind speed in AS (X_1)	0.20	No	No
Wind speed in BoB (X_2)	-0.31	No	No
Wind speed in SIO (X_3)	-0.13	No	No
Wind conv in AS (X_4)	-1.42	No	No
Wind conv in BoB (X_5)	0.06	No	No
Wind conv in SIO (X_6)	1.03	No	No
Wind curl in AS (X_7)	0.74	No	No
Wind curl in BoB (X_8)	-0.34	No	No
Wind curl in SIO (X_9)	0.41	No	No

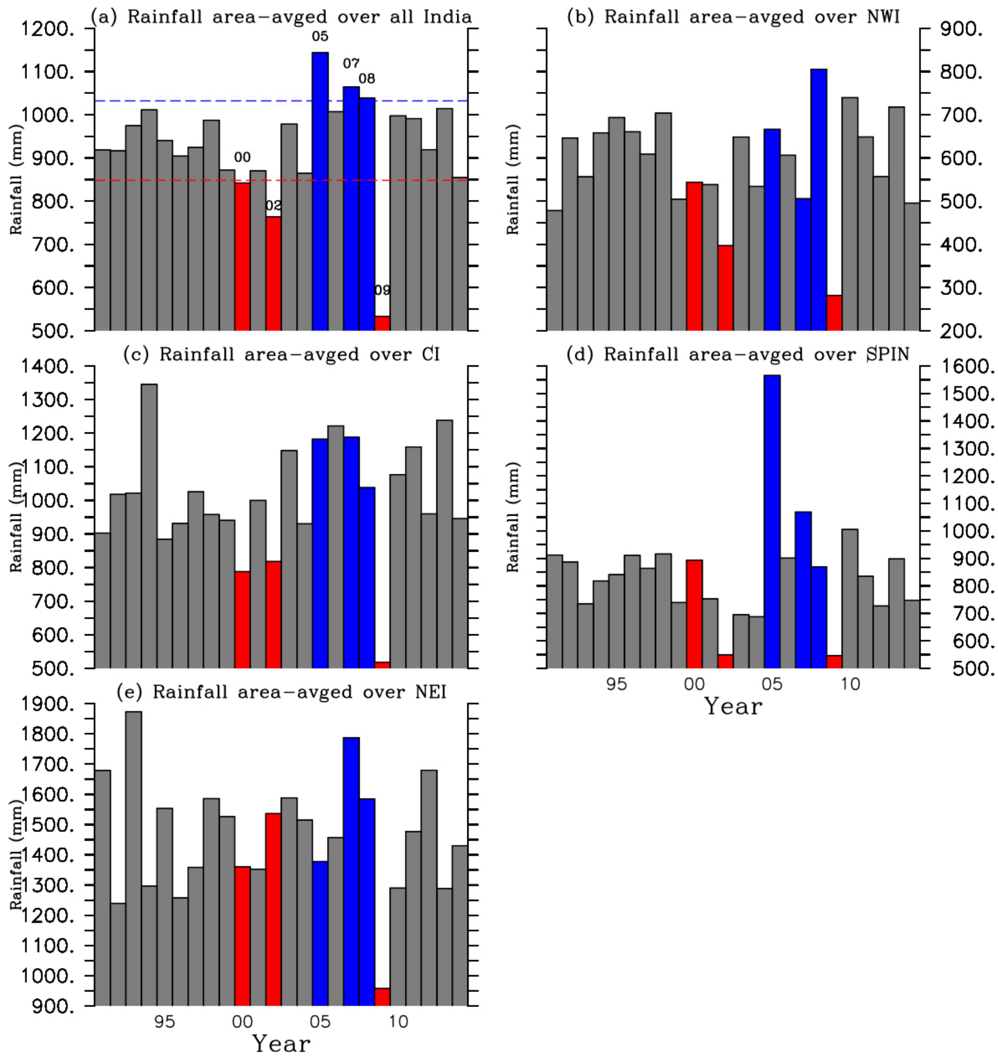

Fig. 1 Evolution of JJAS Indian rainfall (in mm) area-averaged over (a) all India, (b) NWI, (c) CI, (d) SPIN, and (e) NEI during the period 1991–2014 derived from the daily gridded (1°×1°) rainfall product provided by IMD. The JJAS rainfall averaged over all India and the four IMD regions during strong, weak, and normal monsoon years is denoted in blue, red, and gray, respectively. Strong, weak, and normal ISMRs are identified by the departure of JJAS rainfall area-averaged over all India each year from the JJAS rainfall climatology computed (i.e., 938 mm) computed from the daily gridded rainfall over the period 1951–2014, whose departure values are larger than +10%, smaller than –10%, and within –10% and +10% of the seasonally climatology, respectively. The blue (red) dashed line denotes a value of 110% (90%) of seasonal climatology (i.e., the mean climatology is 938 mm), which is 1031 mm (844 mm). The years of strong and weak ISMRs are denoted by the numbers over the bars in panel (a).

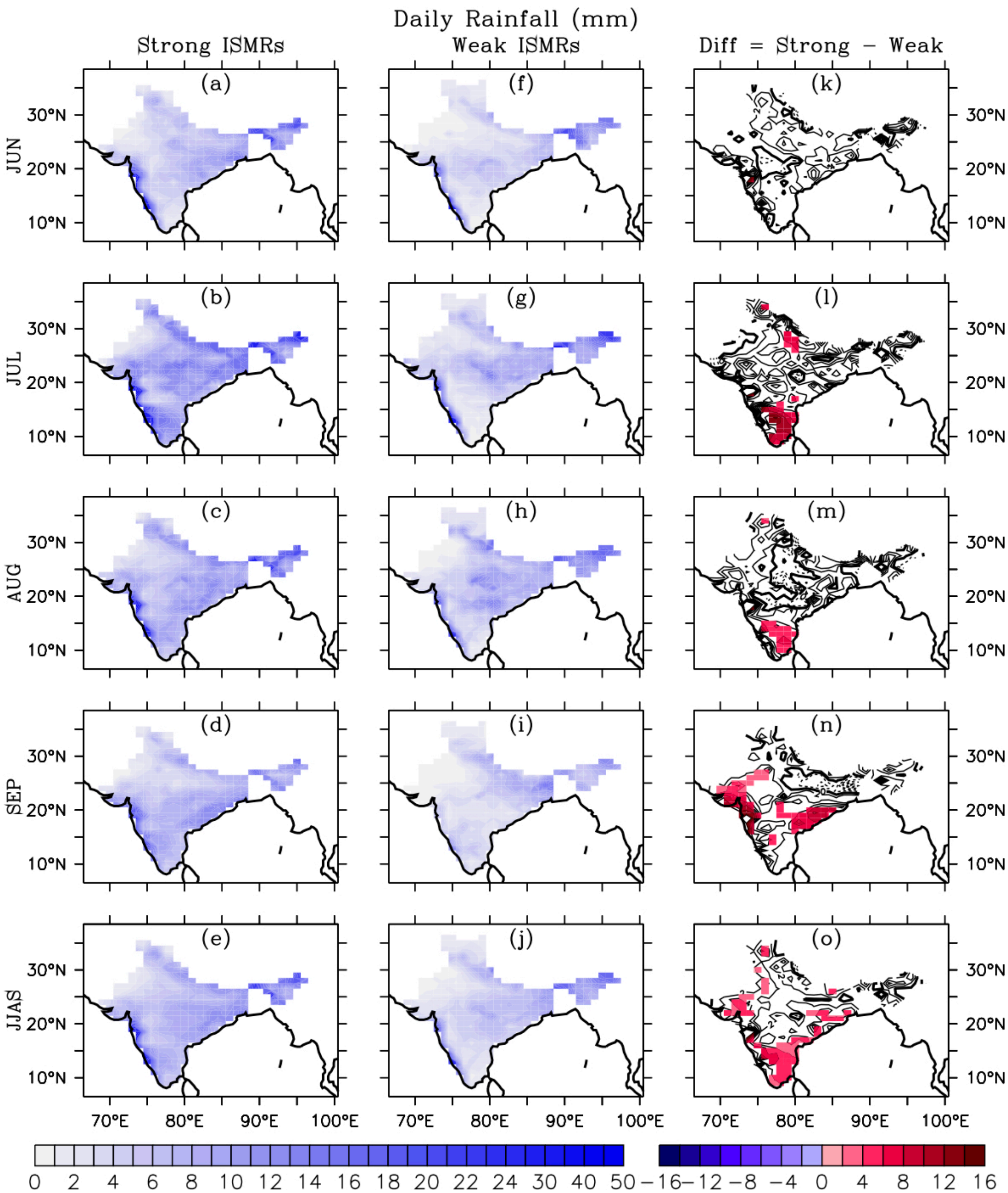

Fig. 2 Geographic distribution of monthly and seasonally averaged rainfall derived from daily rainfall (in mm) during strong and weak ISMRs as well as their corresponding differences (rainfall during strong ISMR years minus rainfall during weak ISMR years) between strong and weak ISMR years. The statistically significant differences at the 99% confidence level are shaded. The left (right) color bar is for time mean (difference) values.

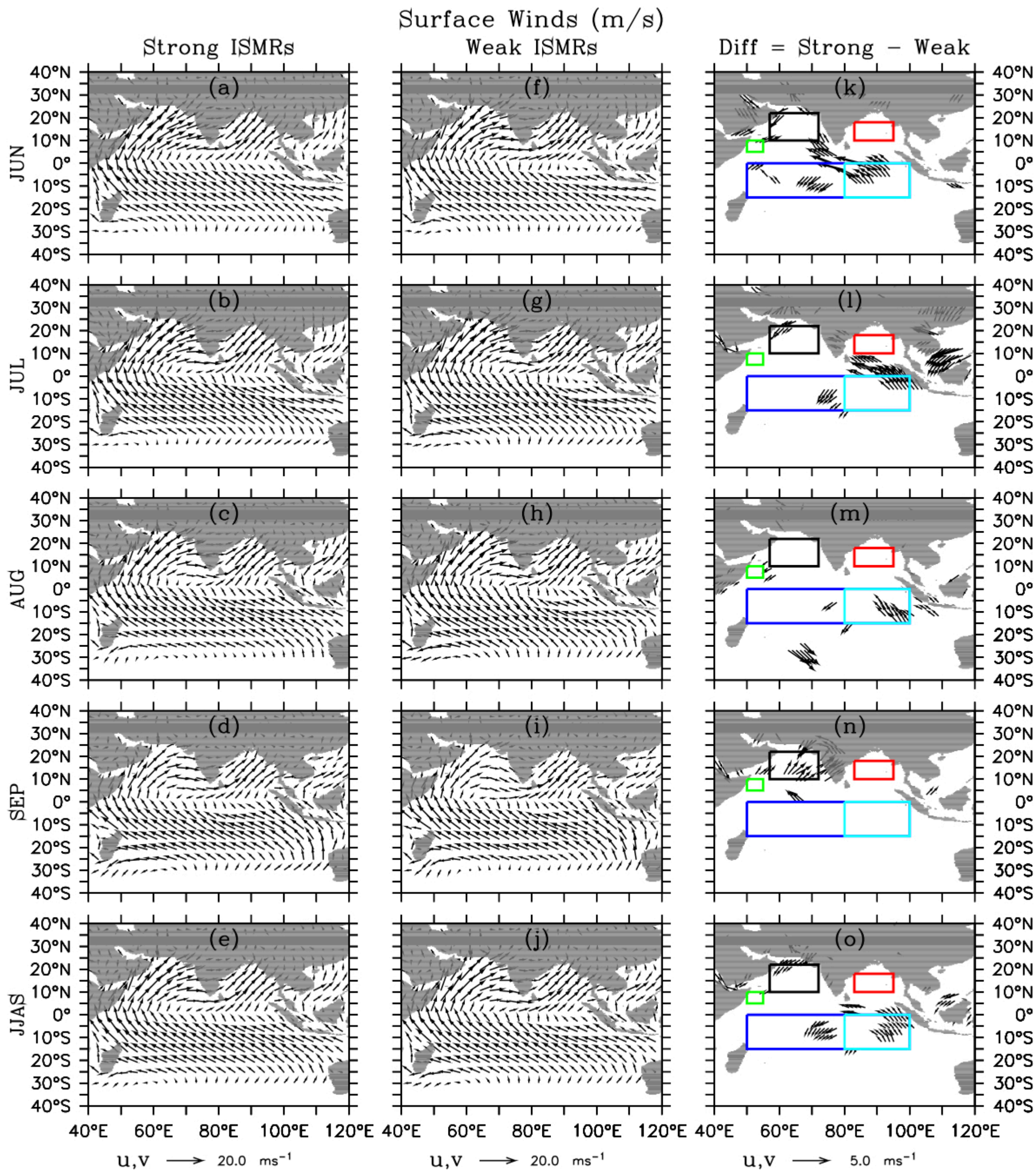

Fig. 3 Same as Fig. 2 except for surface wind vector in the Indian Ocean. AS (57°E–72°E, 10°N–22°N), BoB (83°E–95°E, 10°N–18°N), SC (50°E–55°E, 5°N–10°N), EIO (80°E–100°E, 15°S–0°N), and SIO (50°E–100°E, 15°S–0°N) are delimited by a black, red, green, cyan, and blue rectangle, respectively. Unit: m s^{-1}.

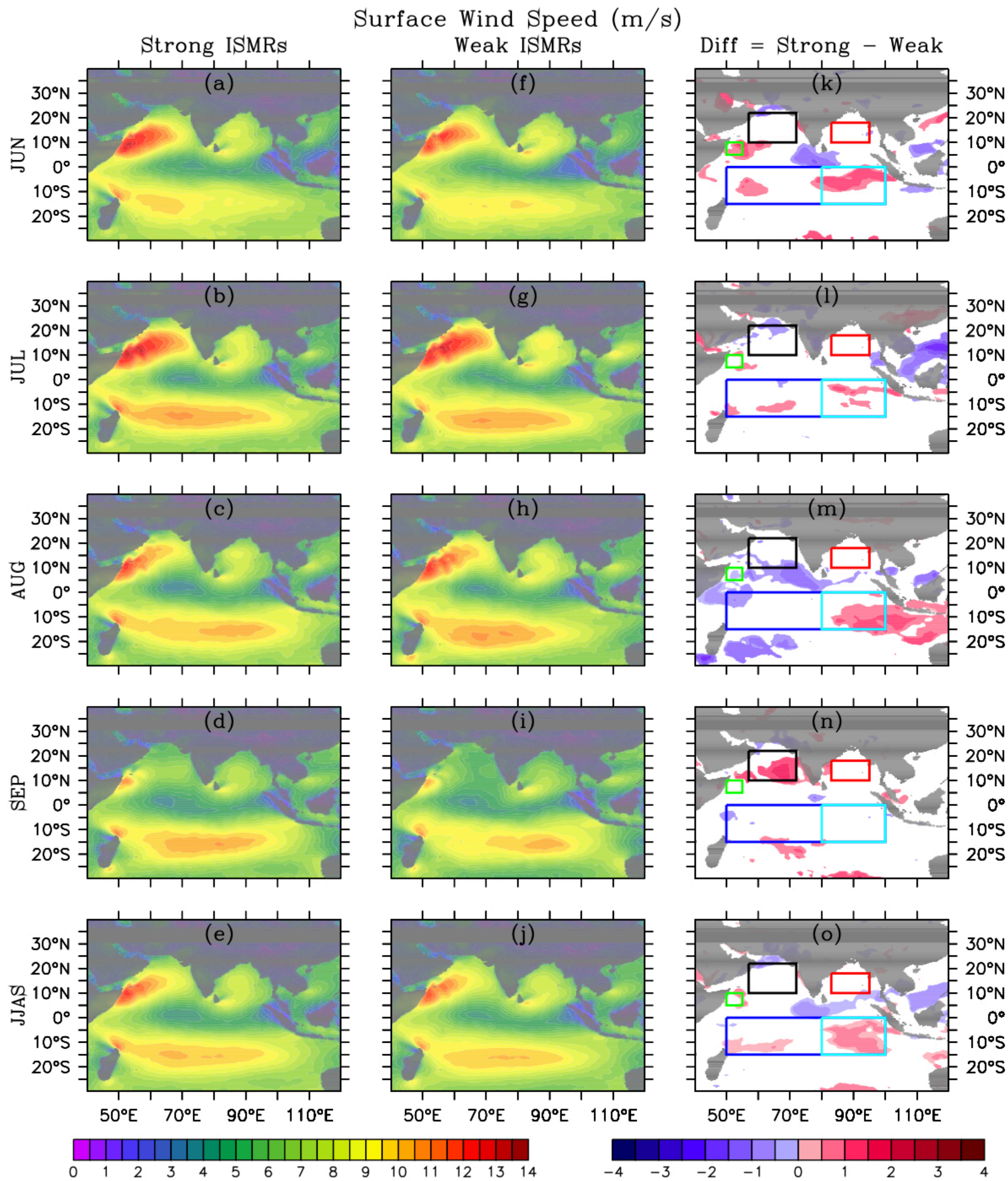

Fig. 4 Same as Fig. 3 except for surface wind speed. The left (right) color bar is for temporal mean (difference) values. Unit: m s^{-1}.

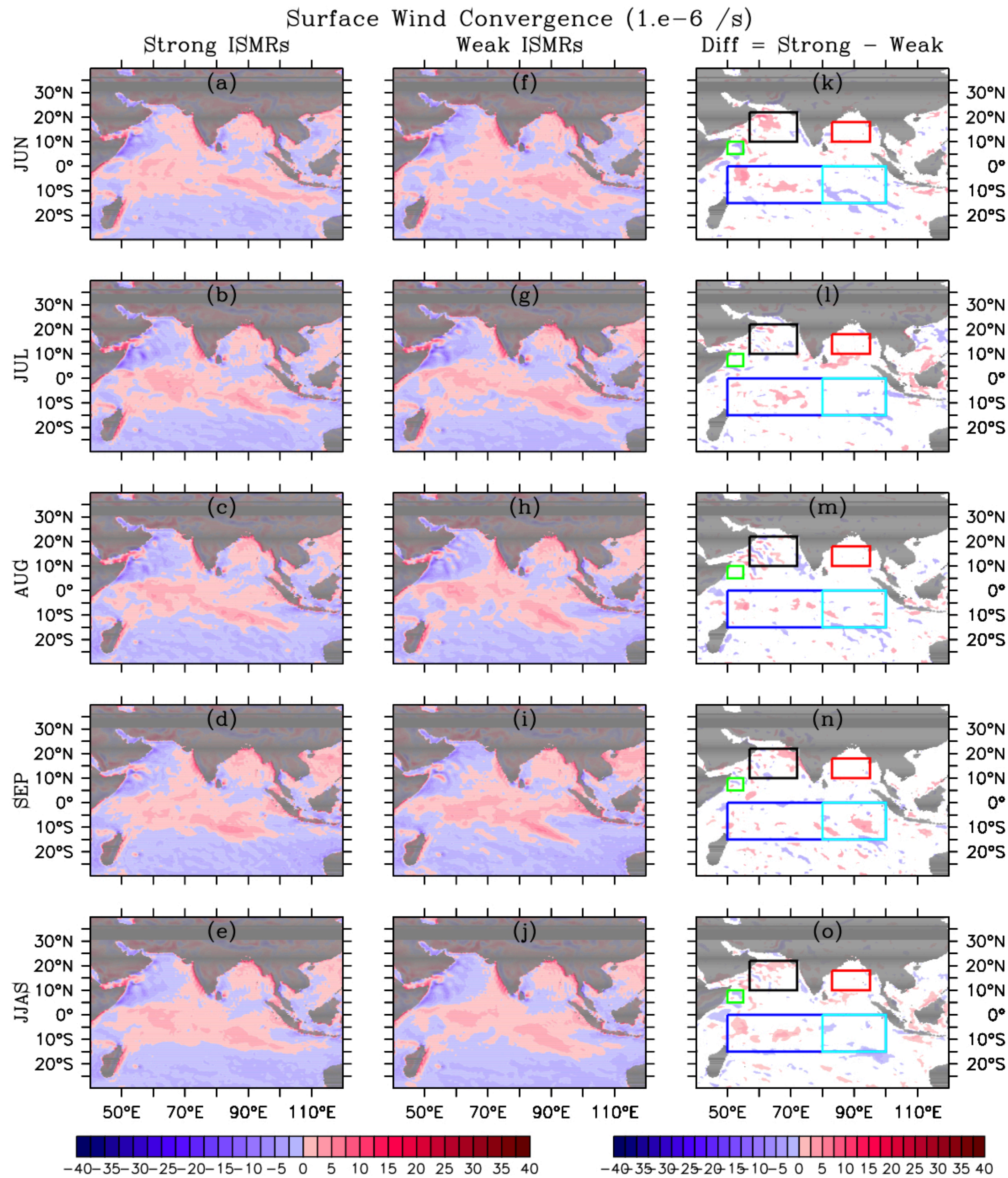

Fig. 5 Same as Fig. 4 except for surface wind convergence. Positive (negative) value on the left two panes denotes surface convergence (divergence). The left (right) color bar is for temporal mean (difference) values. Unit: 10^{-6} s^{-1}.

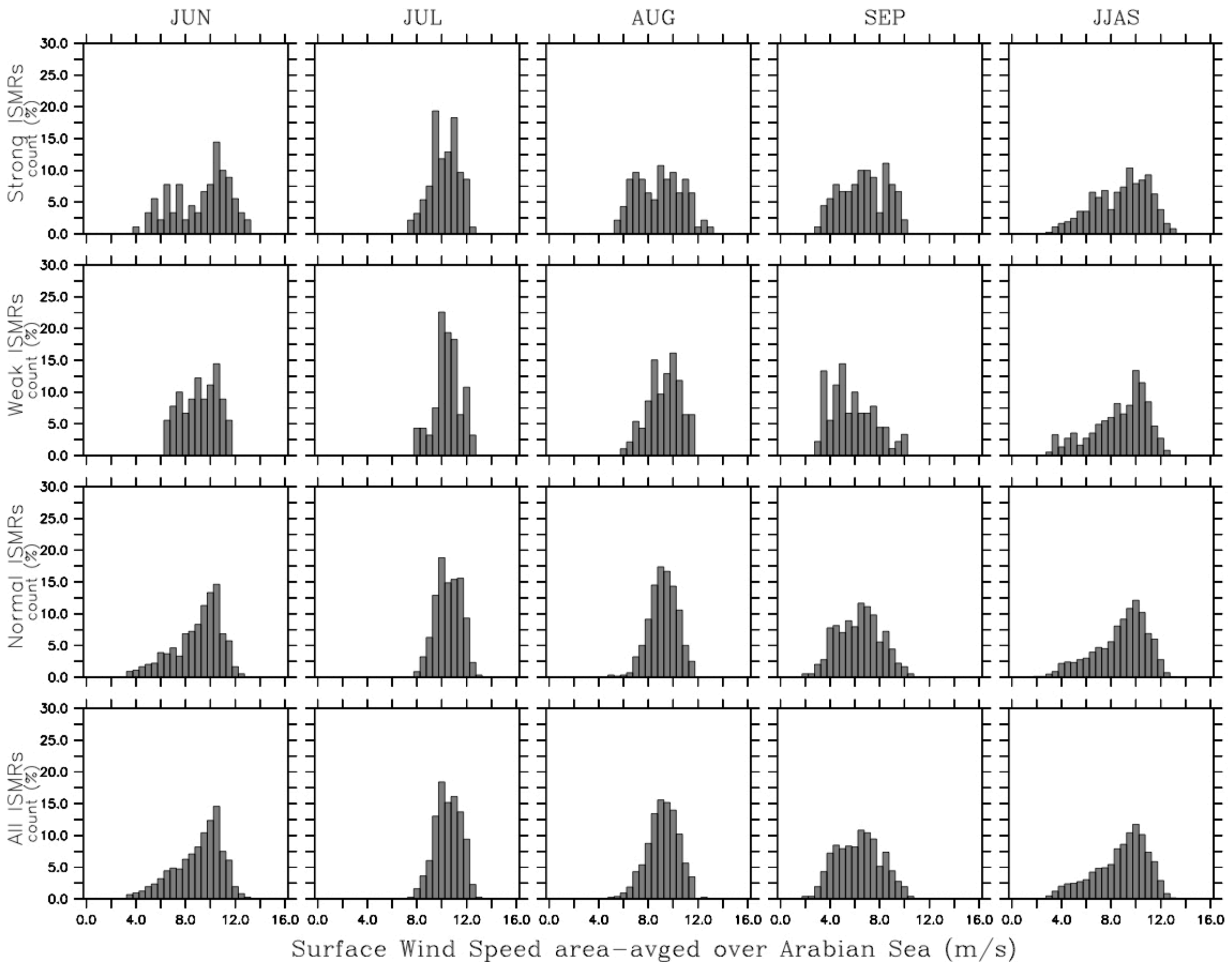

Fig. 6 PDF distribution of daily surface wind speed over the Arabian Sea during strong, weak, normal ISMR years, and across all years (1991–2014). All counts are normalized to 100 for comparison purposes among the months of each ISMR category, so that the integration of the y values over the axis represents the occurring probability (in %) for each surface wind range.

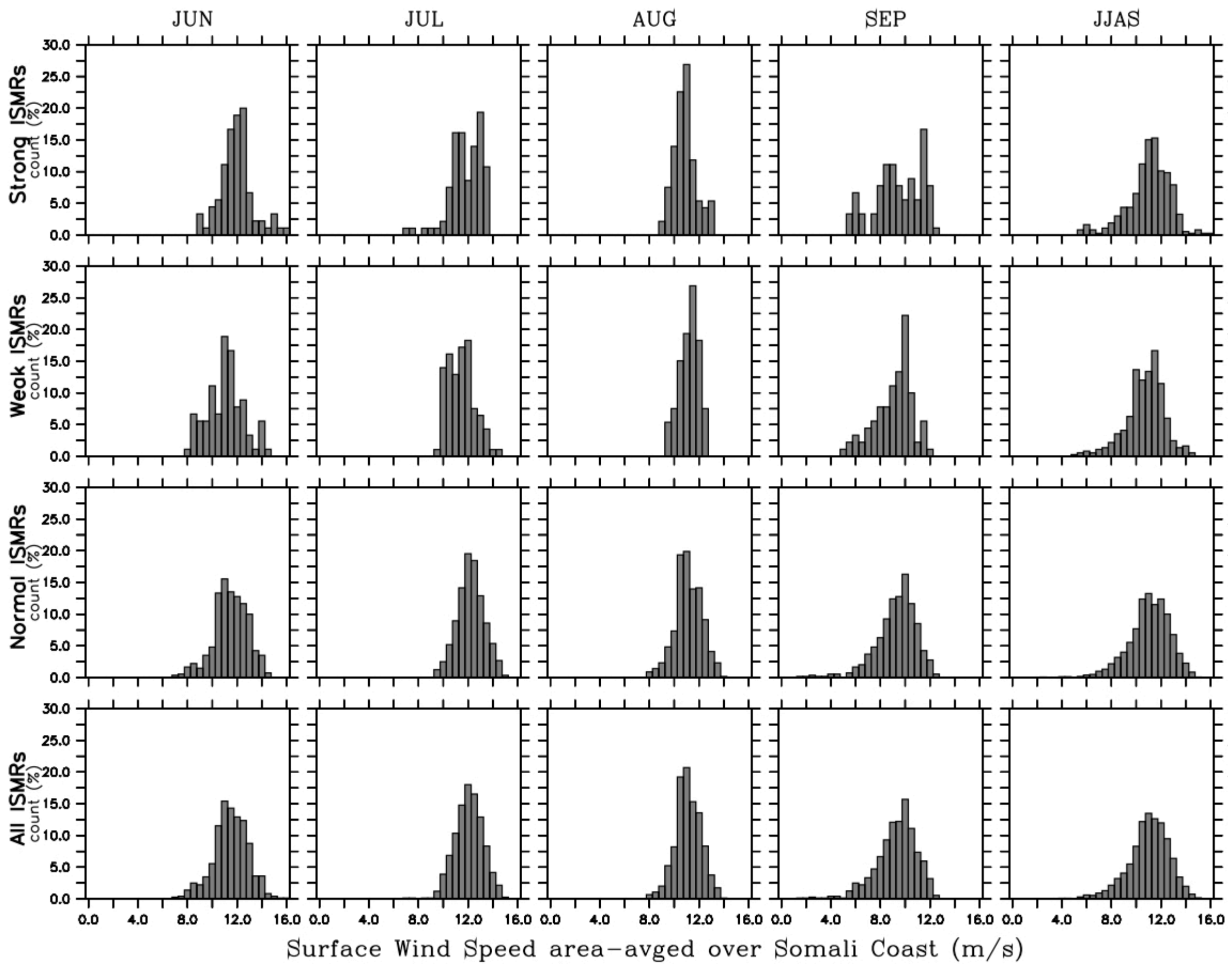

Fig. 7 Same as Fig. 6 except for daily surface wind speed along the Somali coast (SC).

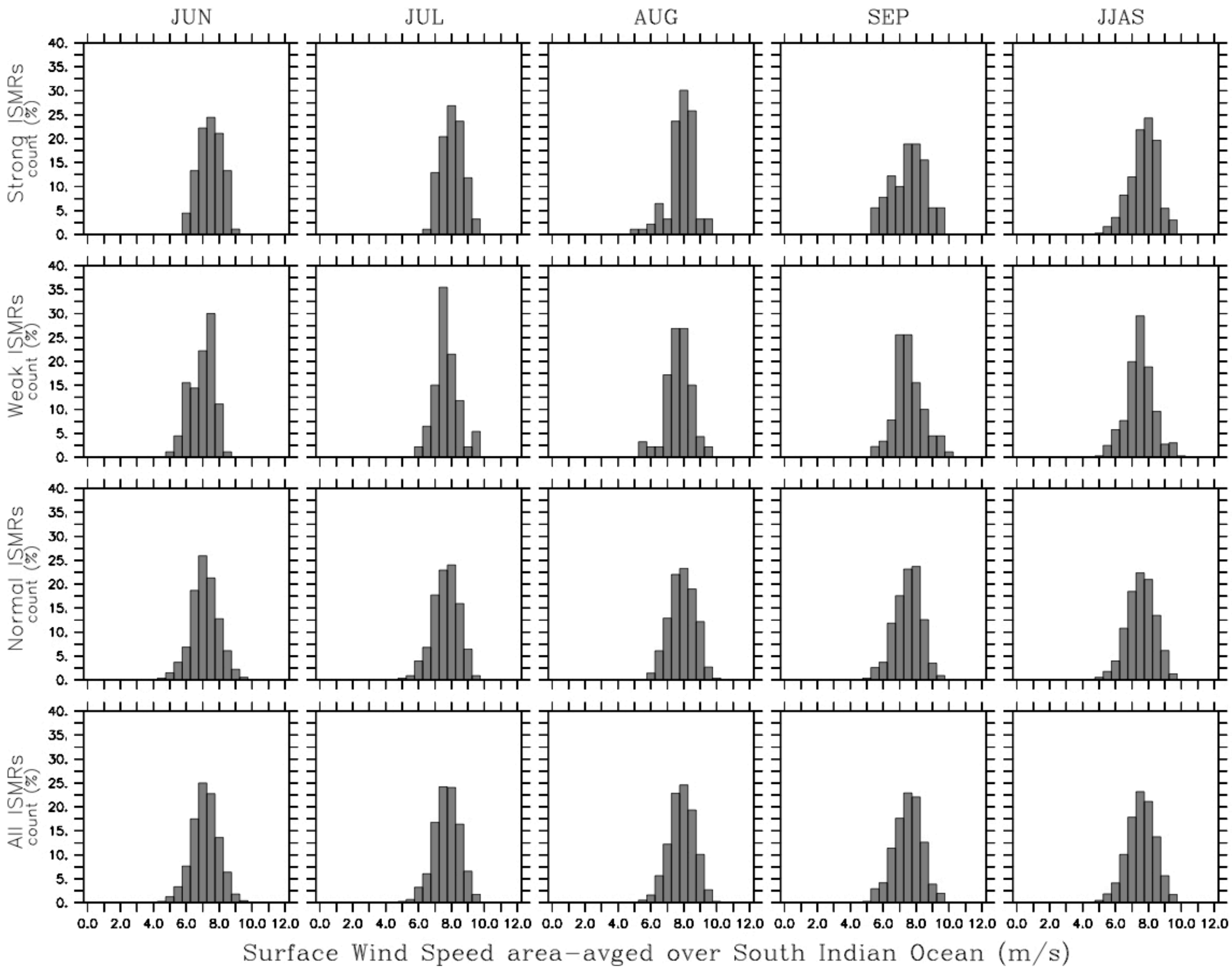

Fig. 8 Same as Fig. 6 except for daily surface wind speed over the Southern Indian Ocean.

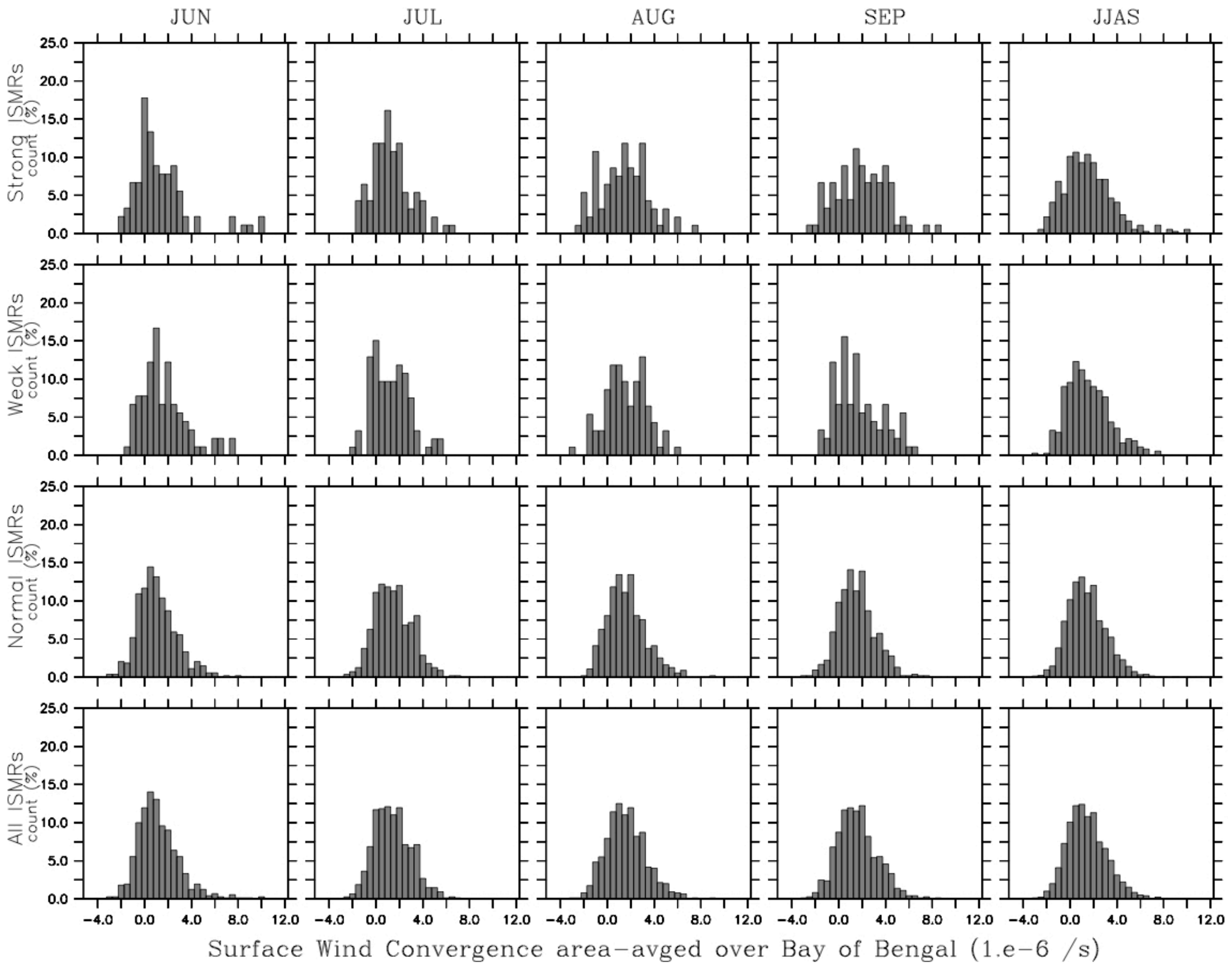

Fig. 9 Same as Fig. 8 except for daily surface wind convergence over the Bay of Bengal.

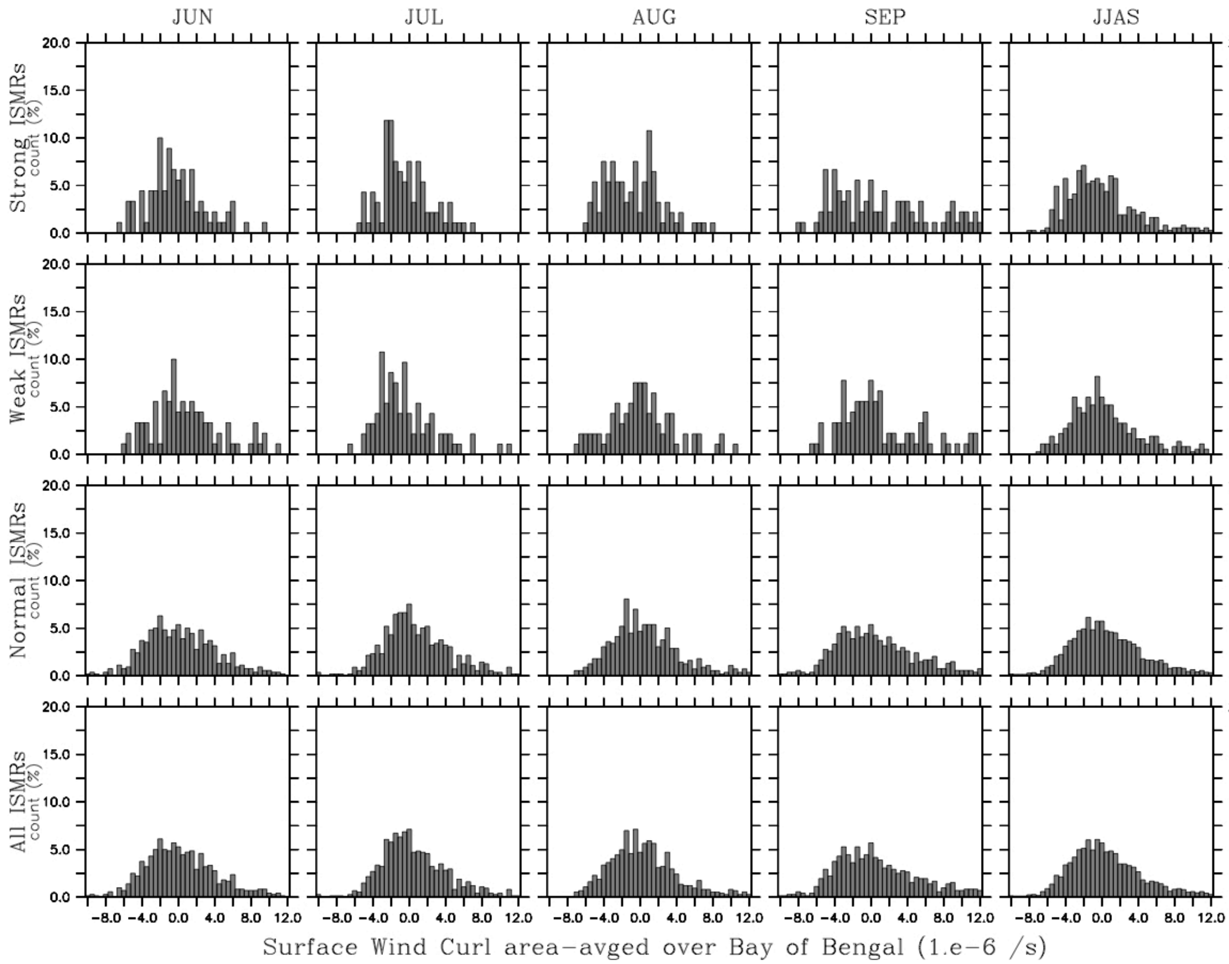

Fig. 10 Same as Fig. 9 except for daily surface wind curl over the Bay of Bengal.

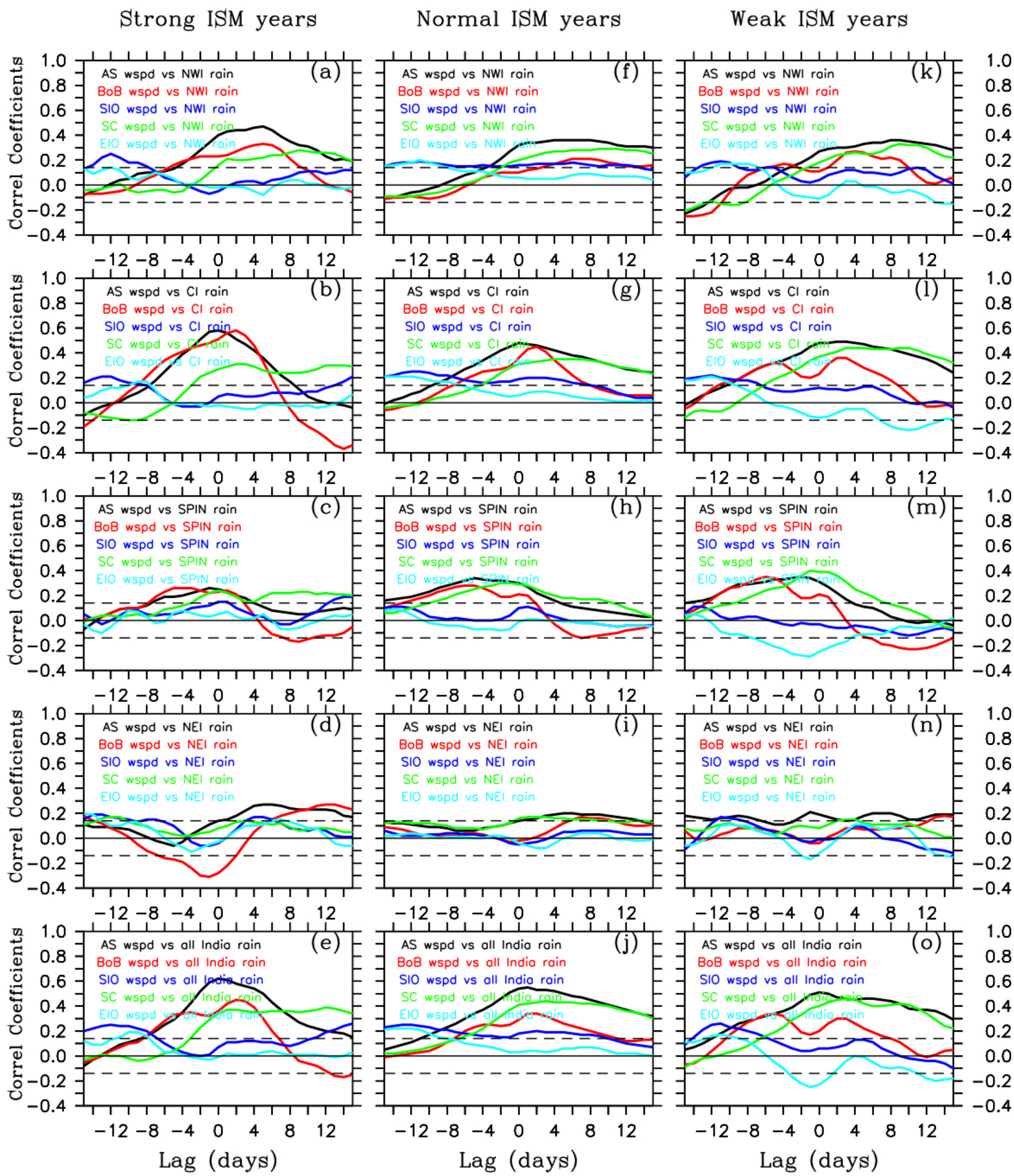

Fig. 11 Lag correlation between daily surface wind speed over the AS, BoB, SIO, SC, EIO and daily rainfall over (a) NWI, (b) CI, (c) SPIN, (d) NEI, (e) all-India during strong ISM years. (f)–(j) and (k)–(o) is the same as (a)–(e) but for normal and weak ISM years, respectively. "+" ("–") days in x-axis denote surface wind speed leads (lags) rainfall.

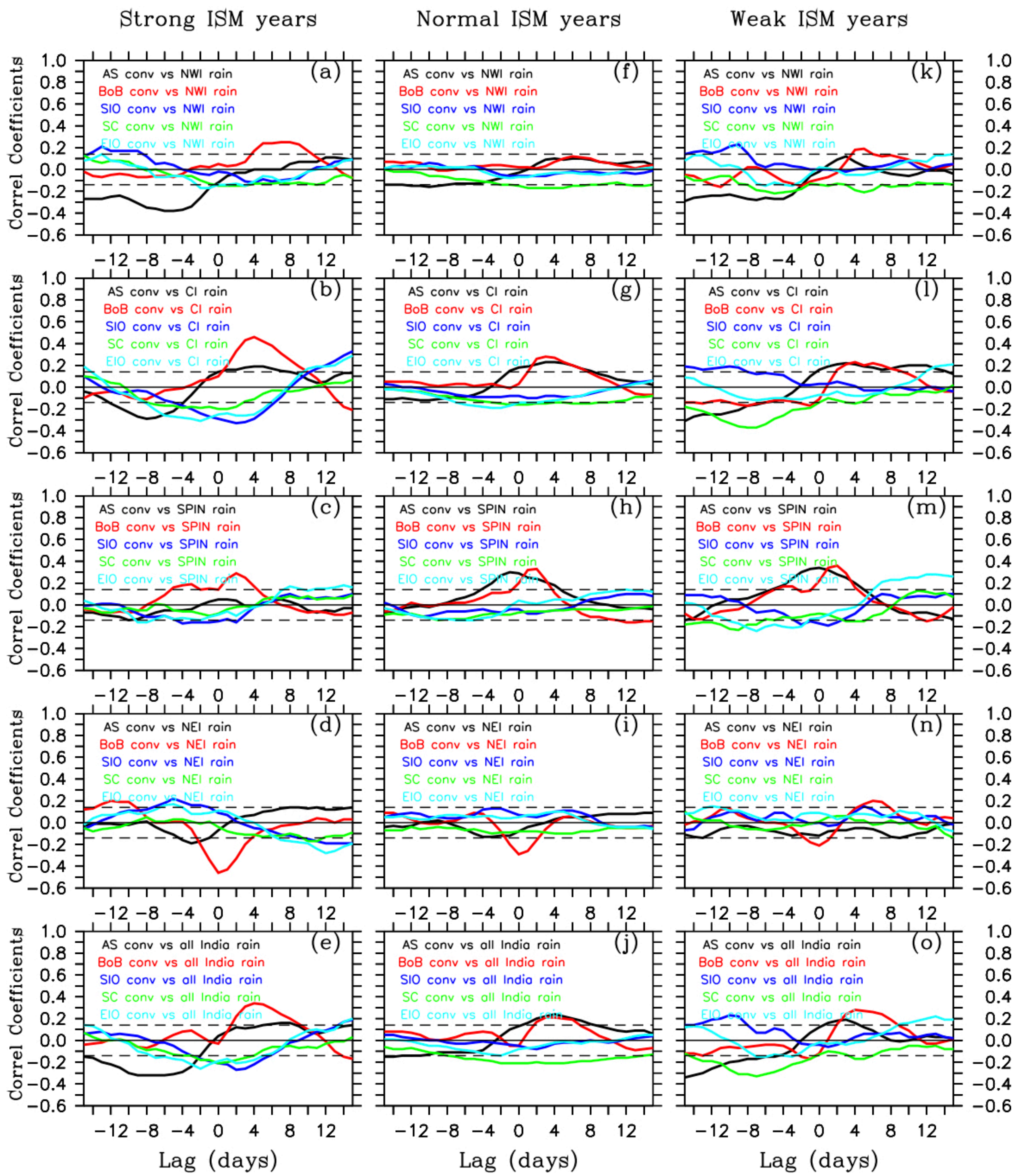

Fig. 12 Same as Fig. 11 except for lag correlation between daily surface wind convergence and daily rainfall.

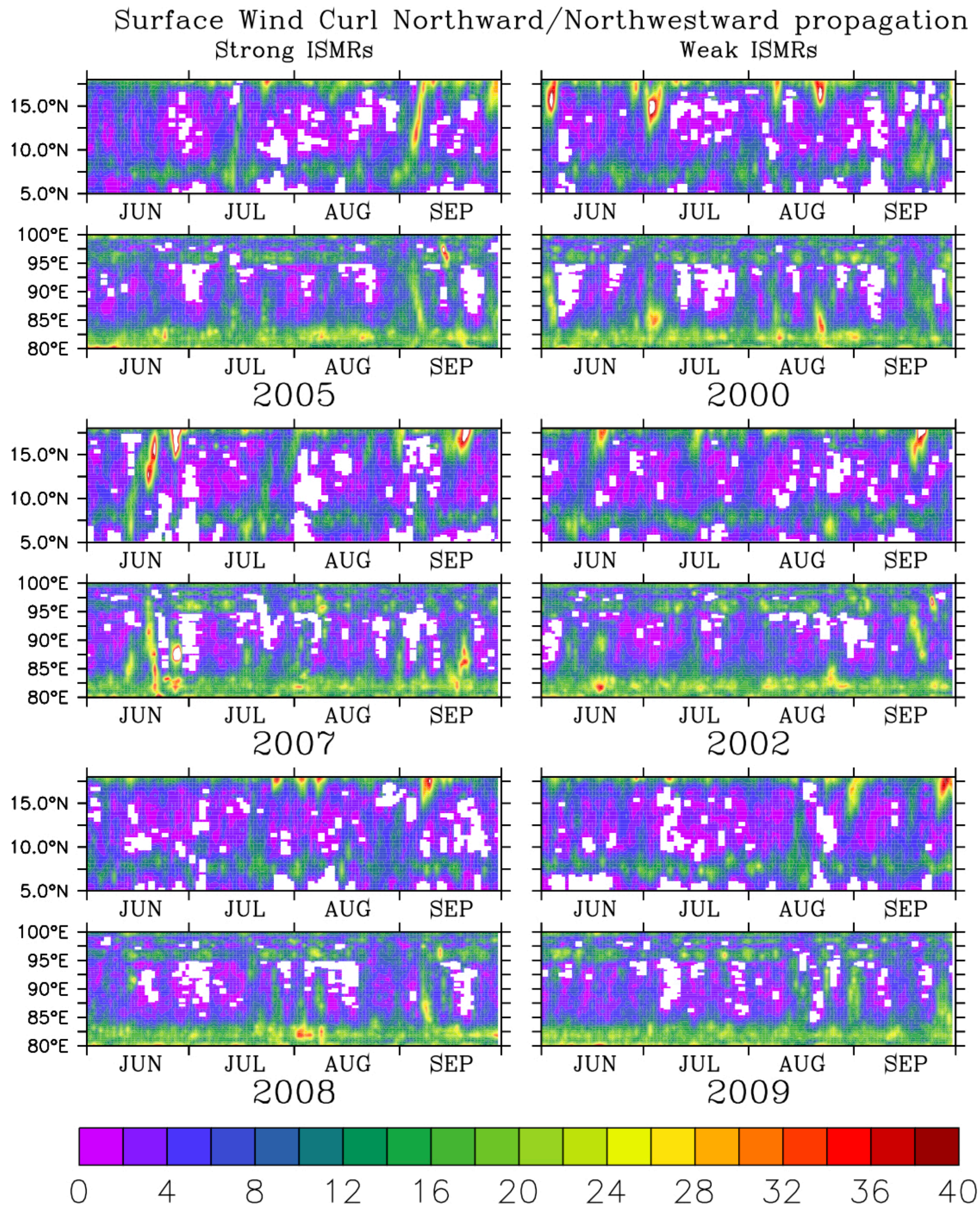

Fig. 13 Time-latitude plot of the daily surface wind curl ($\times 10^{-6}\ s^{-1}$) averaged between 83°E and 95°E (top panel in every year) and time-longitude plot of the daily surface wind curl averaged between 5°N and 10°N (bottom panel in every year) over the Bay of Bengal during strong (left) and weak (right) ISMRs. Plots show only positive values of surface wind curl (representing cyclonic vorticity).

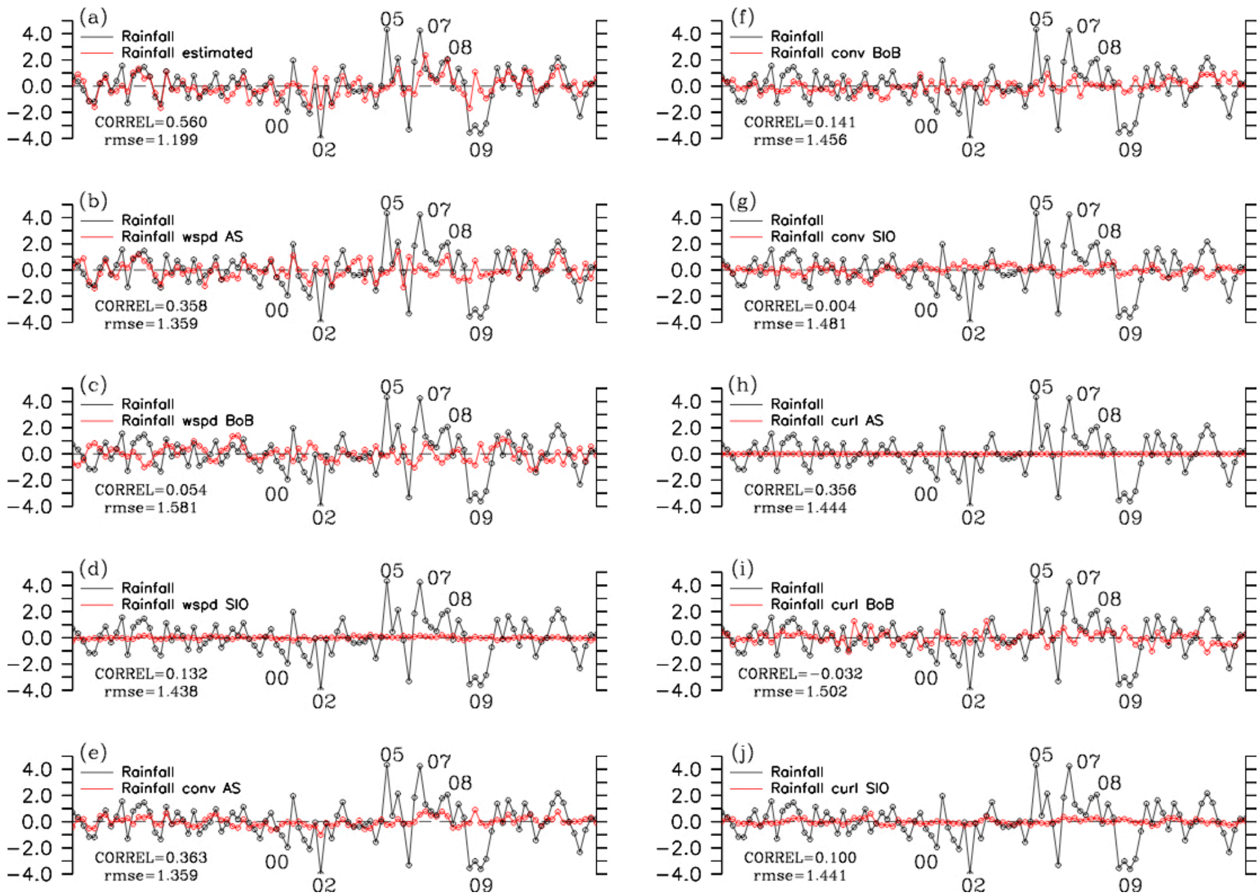

Fig. 14 Anomalous monthly rainfall (in red) in June through September estimated from wind speed, wind convergence, and wind curl in the AS, BoB, and SIO using multiple linear regression model was compared to the actual rainfall (in black). (a) Rainfall estimated from the total nine components; (b) (c), (d) Rainfall estimated from wind speed in the AS, BoB, and SIO, respectively; (e), (f), (g) Rainfall estimated from wind convergence in the AS, BoB, and SIO, respectively; and (h), (i), (j) Rainfall estimated from wind curl in the AS, BoB, and SIO, respectively. Correlation coefficient and root-mean-square error (rmse) for each component are denoted at the left bottom of each panel.